Four-view geometry with unknown radial distortion

Petr Hruby, Viktor Korotynskiy, Timothy Duff, Luke Oeding, Marc Pollefeys, Tomas Pajdla, Viktor Larsson

WED-AM-073

Motivation

- 3D reconstruction **without modelling intrinsics**

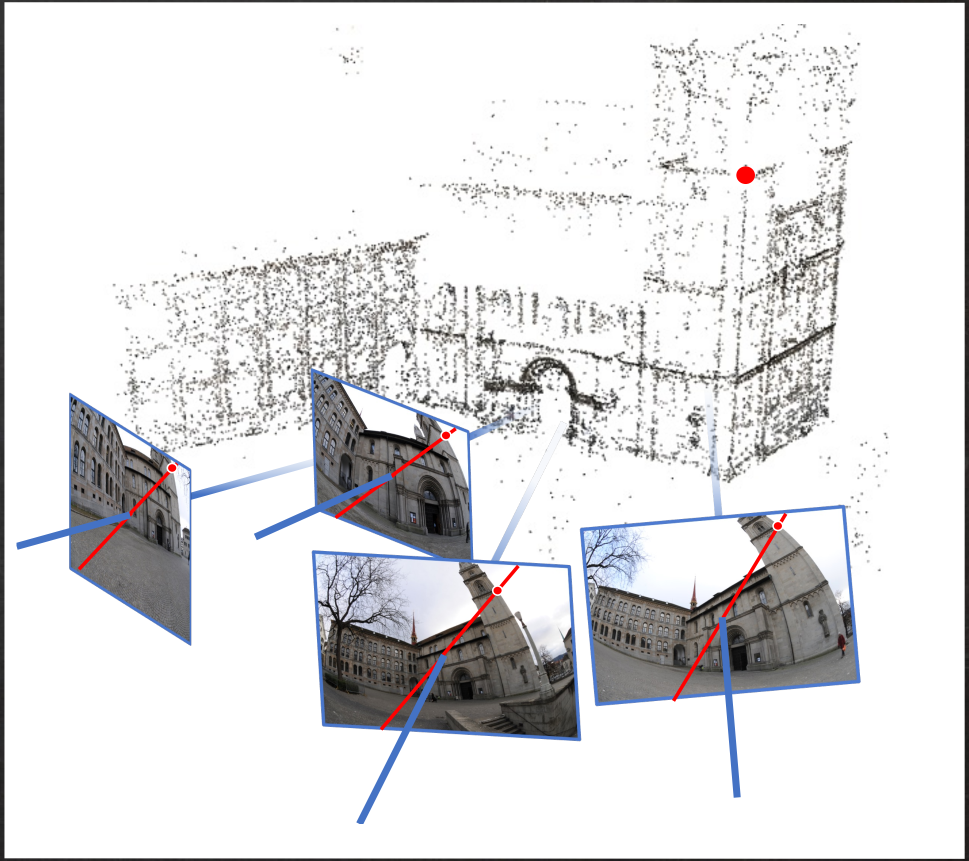

Motivation

- 3D reconstruction **without modelling intrinsics**
- No prior information about the cameras, except for their **radial symmetry**

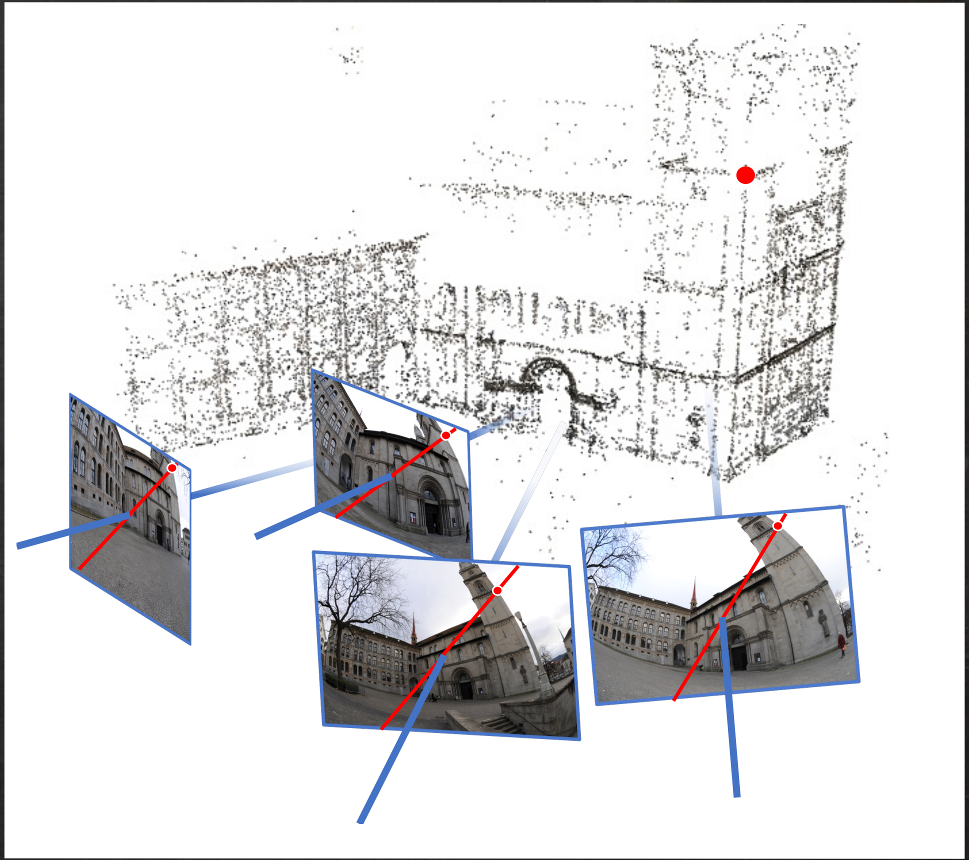

Motivation

- 3D reconstruction **without modelling intrinsics**
- No prior information about the cameras, except for their **radial symmetry**

Motivation

- 3D reconstruction **without modelling intrinsics**
- No prior information about the cameras, except for their **radial symmetry**
- Works for pinhole cameras

Images from: Calibration-free Structure-from-Motion with Calibrated Radial Trifocal Tensors, V. Larsson, N. Zobernig, K. Taskin, M. Pollefeys
Manifold surface reconstruction of an environment from sparse Structure-from-Motion data, M. Lhuillier, S. Yu

Motivation

- 3D reconstruction **without modelling intrinsics**
- No prior information about the cameras, except for their **radial symmetry**
- Works for pinhole cameras, fisheye cameras

Images from: Calibration-free Structure-from-Motion with Calibrated Radial Trifocal Tensors, V. Larsson, N. Zobernig, K. Taskin, M. Pollefeys
Manifold surface reconstruction of an environment from sparse Structure-from-Motion data, M. Lhuillier, S. Yu

Motivation

- 3D reconstruction **without modelling intrinsics**
- No prior information about the cameras, except for their **radial symmetry**
- Works for pinhole cameras, fisheye cameras, catadioptric cameras, ...

Images from: Calibration-free Structure-from-Motion with Calibrated Radial Trifocal Tensors, V. Larsson, N. Zobernig, K. Taskin, M. Pollefeys
Manifold surface reconstruction of an environment from sparse Structure-from-Motion data, M. Lhuillier, S. Yu

Contributions

- Minimal problem: relative pose between **4 radial cameras** from **13 point correspondences**.

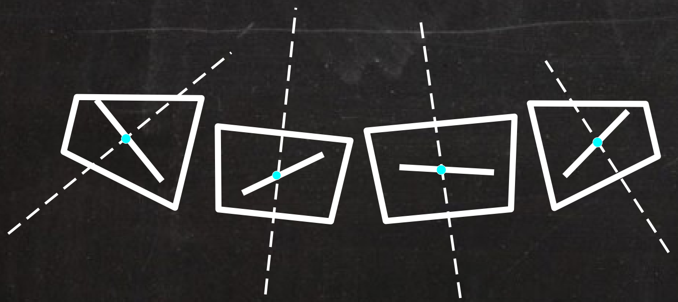

Contributions

- Minimal problem: relative pose between **4 radial cameras** from **13 point correspondences**.
- Study of this minimal problem:
  - 3584 solutions
  - decomposes into subproblems with 28, 2, 4, 2, 2, 2, and 2 solutions

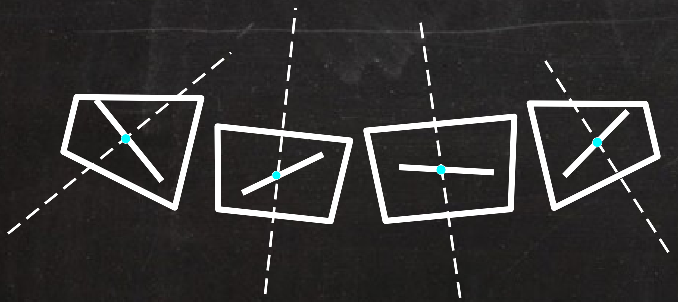

Contributions

- Minimal problem: relative pose between **4 radial cameras** from **13 point correspondences**.
- Study of this minimal problem:
  - 3584 solutions
  - decomposes into subproblems with 28, 2, 4, 2, 2, 2, and 2 solutions
- **Internal constraints** on the radial quadrifocal tensor

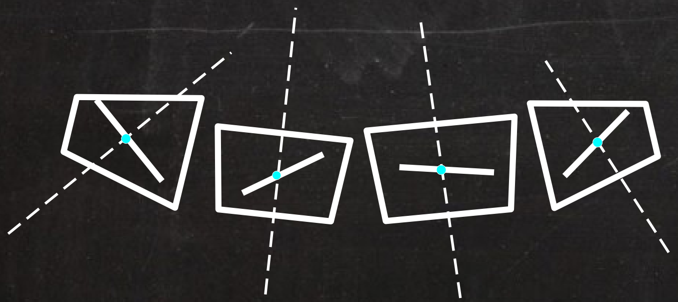

Contributions

- Minimal problem: relative pose between **4 radial cameras** from **13 point correspondences**.
- Study of this minimal problem:
  - 3584 solutions
  - decomposes into subproblems with 28, 2, 4, 2, 2, 2, and 2 solutions
- **Internal constraints** on the radial quadrifocal tensor
- Practical **minimal solver** for the problem

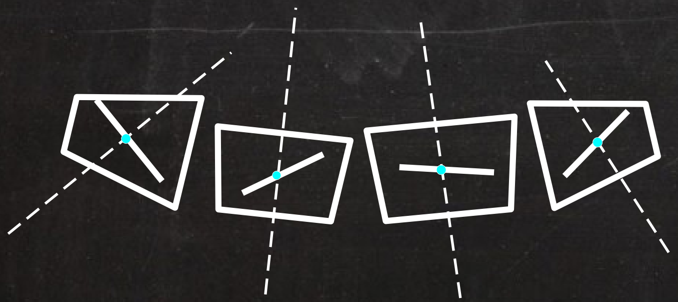

Contributions

- Minimal problem: relative pose between **4** **upright** **radial cameras** from **7 point correspondences**.

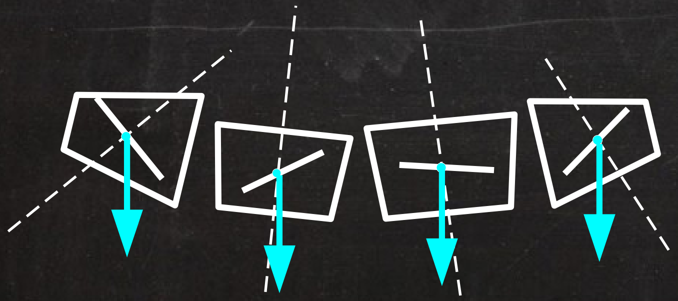

Contributions

- Minimal problem: relative pose between **4 upright radial cameras** from **7 point correspondences**.
- Study of this minimal problem:
  - 50 solutions
  - decomposes into subproblems with 25, and 2 solutions

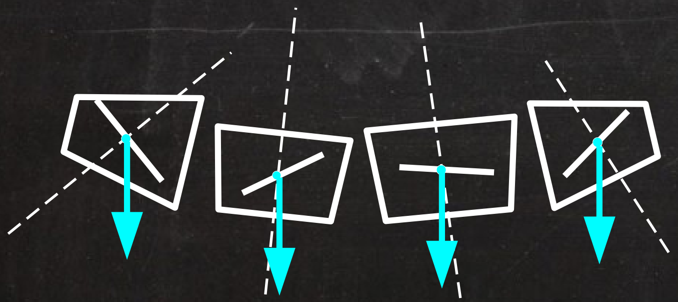

Contributions

- Minimal problem: relative pose between **4** **upright** **radial cameras** from **7 point correspondences**.
- Study of this minimal problem:
  - 50 solutions
  - decomposes into subproblems with 25, and 2 solutions
- Practical **minimal solver** for the problem

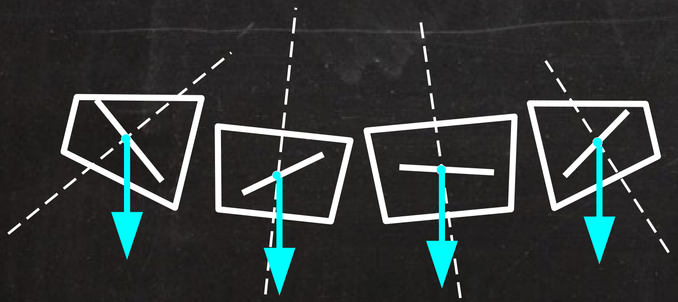

Radial distortion

- Projections $\mathbf{p}$ by the pinhole camera and $\mathbf{p_d}$ by the radially distorted camera lie on the same radial line $\mathbf{l}$.

Radial distortion

- Projections $\mathbf{p}$ by the pinhole camera and $\mathbf{p}_d$ by the radially distorted camera lie on the same radial line $\mathbf{l}$.

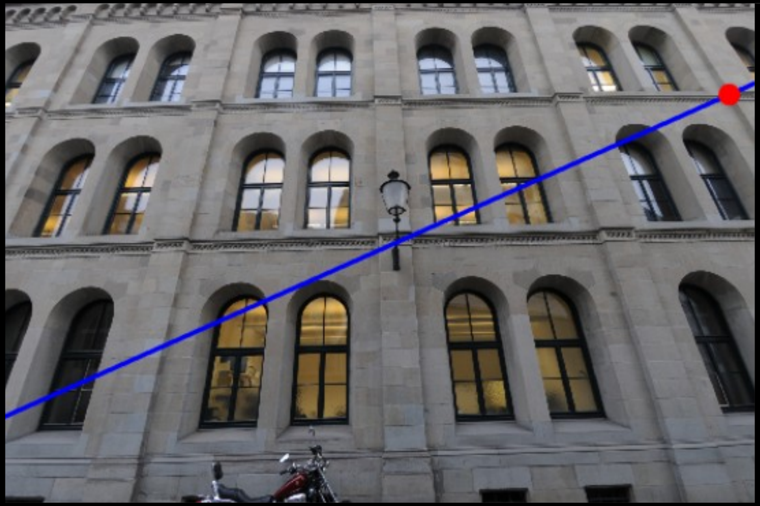

Image: Calibration-free Structure-from-Motion with Calibrated Radial Trifocal Tensors, V. Larsson, N. Zobernig, K. Taskin, M. Pollefeys

Radial distortion

- Projections $\mathbf{p}$ by the pinhole camera and $\mathbf{p}_d$ by the radially distorted camera lie on the same radial line $\mathbf{l}$.

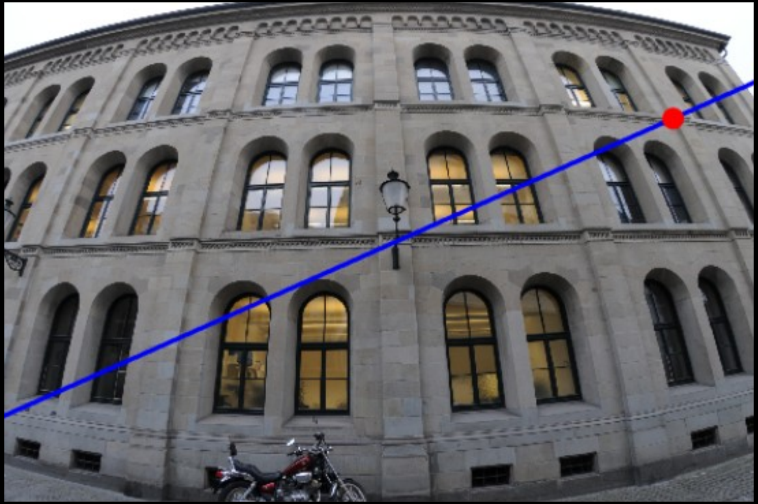

Image: Calibration-free Structure-from-Motion with Calibrated Radial Trifocal Tensors, V. Larsson, N. Zobernig, K. Taskin, M. Pollefeys

Radial distortion

- Projections $\mathbf{p}$ by the pinhole camera and $\mathbf{p_d}$ by the radially distorted camera lie on the same radial line $\mathbf{l}$.

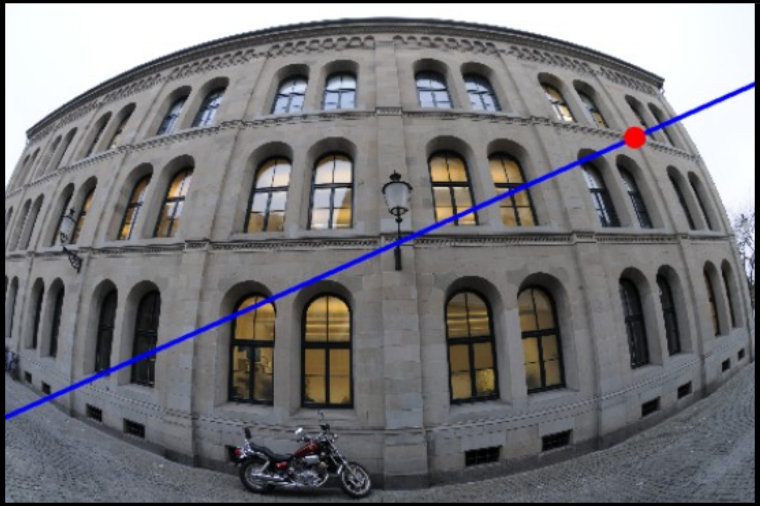

Image: Calibration-free Structure-from-Motion with Calibrated Radial Trifocal Tensors, V. Larsson, N. Zobernig, K. Taskin, M. Pollefeys

Radial distortion

- Projections $\mathbf{p}$ by the pinhole camera and $\mathbf{p_d}$ by the radially distorted camera lie on the same radial line $\mathbf{l}$.

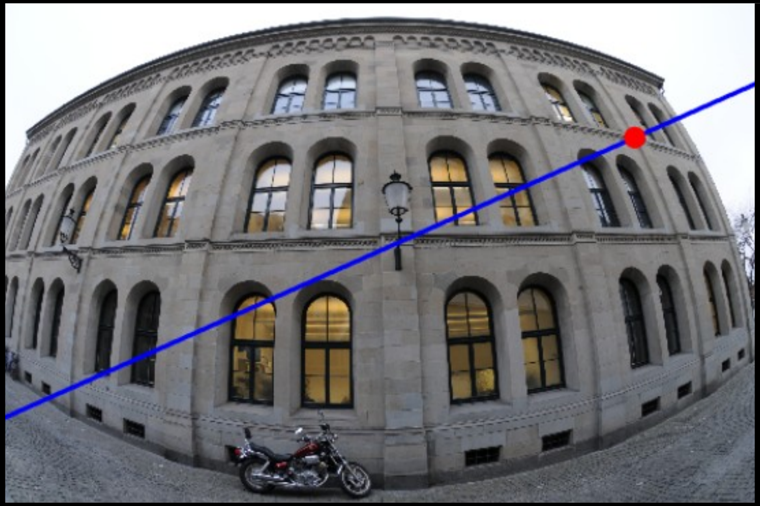

- Models **many real cameras** (fisheye, catadioptric, ...)

Image: Calibration-free Structure-from-Motion with Calibrated Radial Trifocal Tensors, V. Larsson, N. Zobernig, K. Taskin, M. Pollefeys

Radial distortion

- Projections $\mathbf{p}$ by the pinhole camera and $\mathbf{p_d}$ by the radially distorted camera lie on the same radial line $\mathbf{l}$.

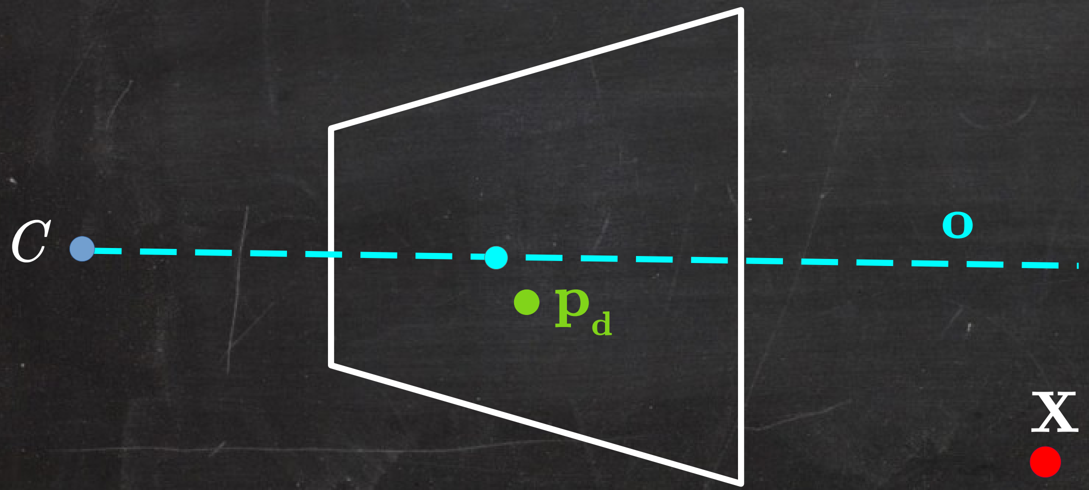

Radial distortion

- Projections $\mathbf{p}$ by the pinhole camera and $\mathbf{p}_d$ by the radially distorted camera lie on the same radial line $\mathbf{l}$.

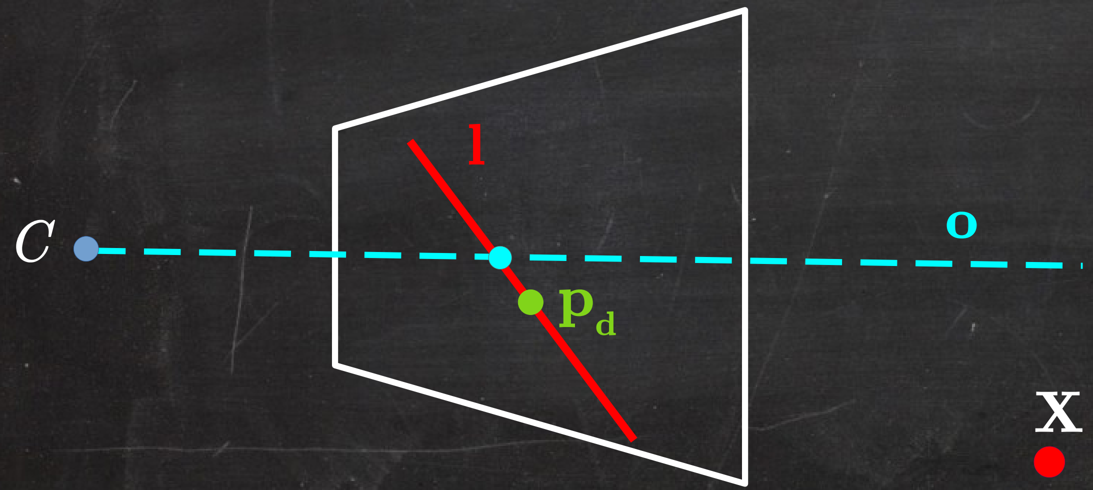

$$\mathbf{l} = \mathbf{p}_d \times \mathbf{o}$$

Radial distortion

- Projections $\mathbf{p}$ by the pinhole camera and $\mathbf{p}_d$ by the radially distorted camera lie on the same radial line $\mathbf{l}$.

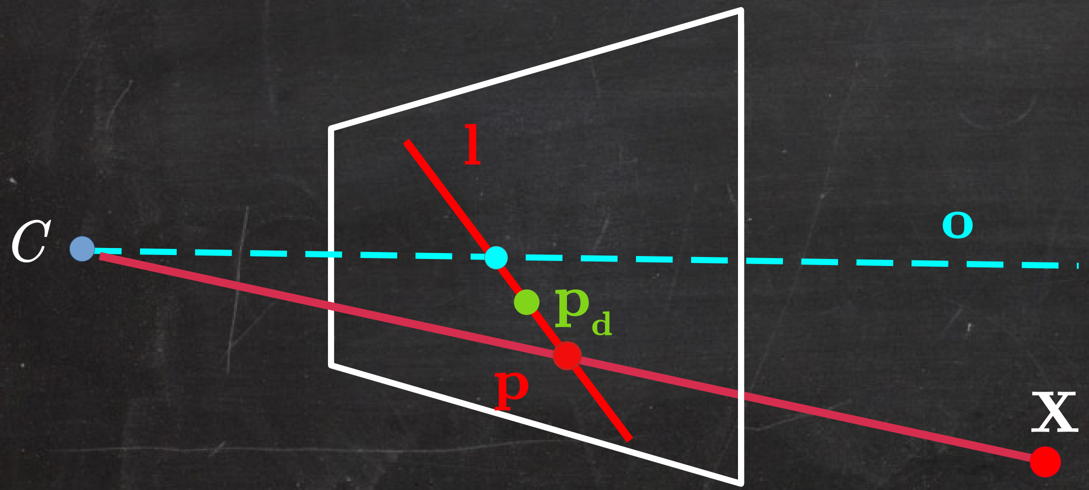

$$\mathbf{l} = \mathbf{p}_d \times \mathbf{o}$$

$$\mathbf{p} \sim \mathrm{R}\mathbf{X}+\mathrm{t}$$

Radial distortion

- Projections $\mathbf{p}$ by the pinhole camera and $\mathbf{p}_d$ by the radially distorted camera lie on the same radial line $\mathbf{l}$.

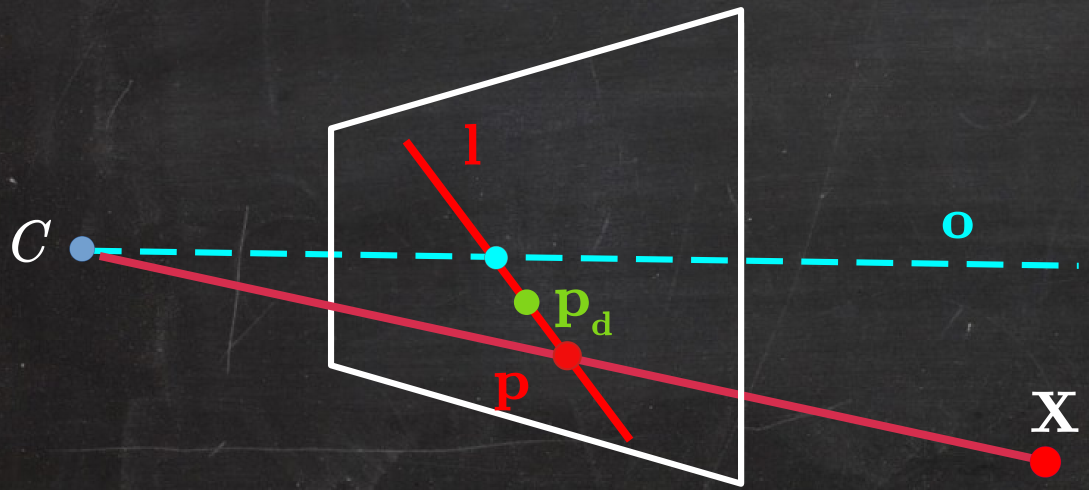

$$\mathbf{l} = \mathbf{p}_d \times \mathbf{o}$$

$$\mathbf{p} \sim \mathrm{R}\mathbf{X} + \mathrm{t}$$

$$\mathbf{l}^T \mathbf{p} = 0$$

Radial distortion

- Projections $\mathbf{p}$ by the pinhole camera and $\mathbf{p}_d$ by the radially distorted camera lie on the same radial line $\mathbf{l}$.

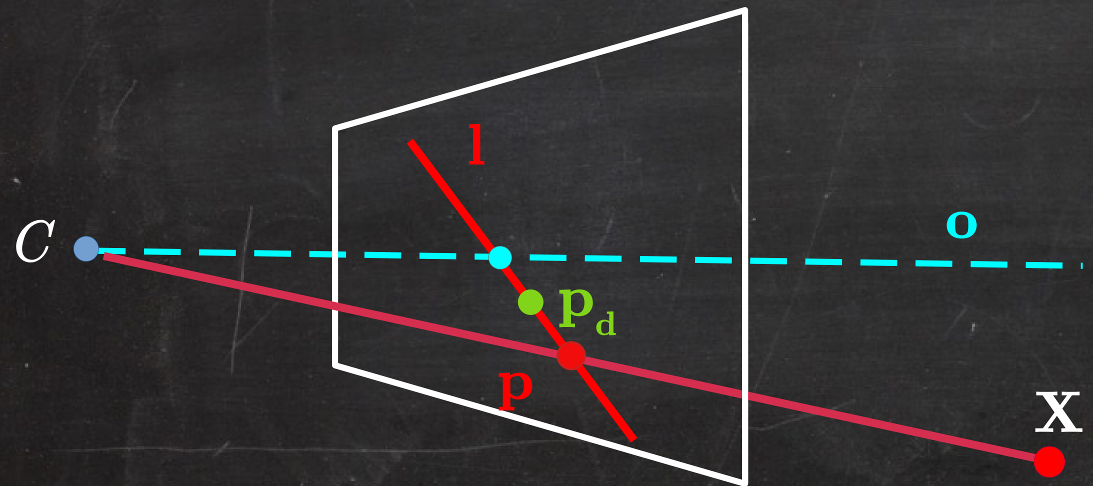

$$\mathbf{l} = \mathbf{p}_d \times \mathbf{o}$$

$$\mathbf{p} \sim \mathrm{R}\mathbf{X}+\mathrm{t}$$

$$\mathbf{l}^T\mathbf{p}=0$$

$$\mathbf{l}^T(\mathrm{R}\mathbf{X}+\mathrm{t})=0$$

Radial distortion

- Projections $\mathbf{p}$ by the pinhole camera and $\mathbf{p_d}$ by the radially distorted camera lie on the same radial line $\mathbf{l}$.

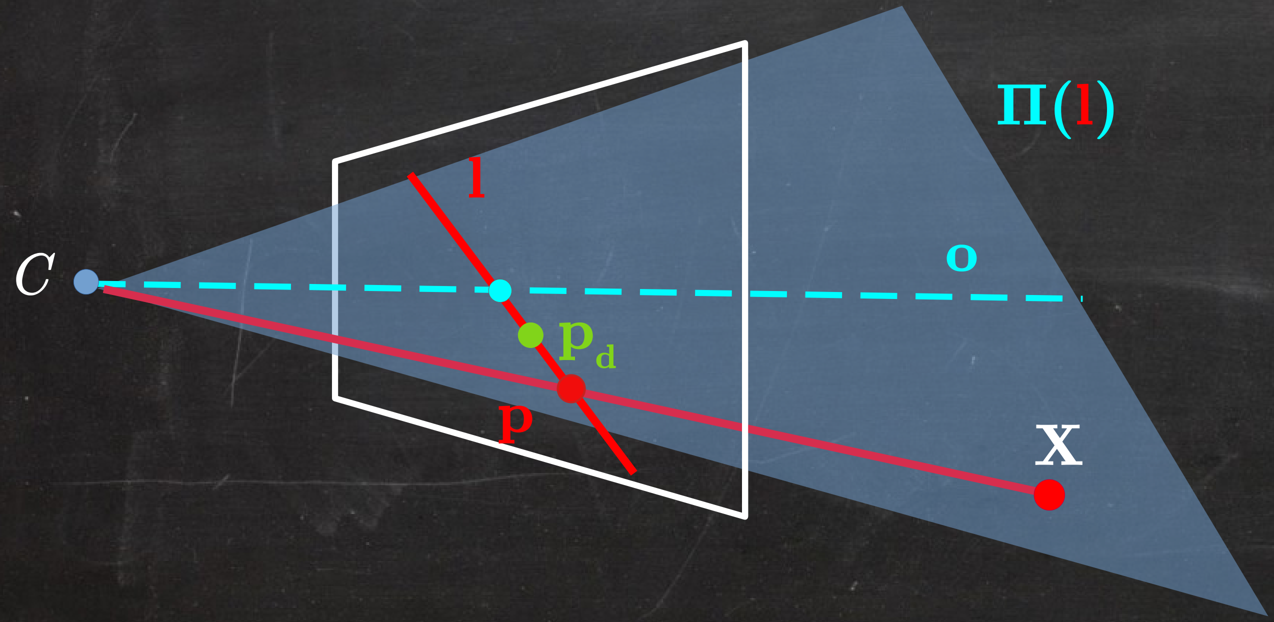

$$\mathbf{l} = \mathbf{p_d} \times \mathbf{o}$$

$$\mathbf{p} \sim \mathrm{R}\mathbf{X}+\mathrm{t}$$

$$\mathbf{l}^T\mathbf{p}=0$$

$$\mathbf{l}^T(\mathrm{R}\mathbf{X}+\mathrm{t})=0$$

$$\mathbf{X} \in \mathbf{\Pi}(\mathbf{l})$$

Radial distortion

- Projections $\mathbf{p}$ by the pinhole camera and $\mathbf{p}_d$ by the radially distorted camera lie on the same radial line $\mathbf{l}$.
- The constraint can be written as $\mathbf{l}^T(\mathrm{R}\mathbf{X}+\mathbf{t})=0$

Radial distortion

- Projections $\mathbf{p}$ by the pinhole camera and $\mathbf{p_d}$ by the radially distorted camera lie on the same radial line $\mathbf{l}$.
- The constraint can be written as $\mathbf{l}^T(\mathbf{R}\mathbf{X}+\mathbf{t})=0$

$$\begin{bmatrix} l_1 & l_2 & l_3 \end{bmatrix} \cdot \left(\begin{bmatrix} R_{11} & R_{12} & R_{13} \\ R_{21} & R_{22} & R_{23} \\ R_{31} & R_{32} & R_{33} \end{bmatrix} \cdot \begin{bmatrix} X_1 \\ X_2 \\ X_3 \end{bmatrix} + \begin{bmatrix} t_1 \\ t_2 \\ t_3 \end{bmatrix} \right) = 0$$

Radial distortion

- Projections $\mathbf{p}$ by the pinhole camera and $\mathbf{p}_d$ by the radially distorted camera lie on the same radial line $\mathbf{l}$.
- The constraint can be written as $\mathbf{l}^T(\mathbf{R}\mathbf{X}+\mathbf{t})=0$

$$\begin{bmatrix} l_1 & l_2 & 0 \end{bmatrix} \cdot \left(\begin{bmatrix} R_{11} & R_{12} & R_{13} \\ R_{21} & R_{22} & R_{23} \\ R_{31} & R_{32} & R_{33} \end{bmatrix} \cdot \begin{bmatrix} X_1 \\ X_2 \\ X_3 \end{bmatrix} + \begin{bmatrix} t_1 \\ t_2 \\ t_3 \end{bmatrix} \right) = 0$$

$\mathbf{l}$ is a radial line passing through the origin

Radial distortion

- Projections $\mathbf{p}$ by the pinhole camera and $\mathbf{p}_d$ by the radially distorted camera lie on the same radial line $\mathbf{l}$.
- The constraint can be written as $\mathbf{l}^T(\mathrm{R}\mathbf{X}+\mathbf{t})=0$

$$\begin{bmatrix} l_1 & l_2 \end{bmatrix} \cdot \left(\begin{bmatrix} R_{11} & R_{12} & R_{13} \\ R_{21} & R_{22} & R_{23} \end{bmatrix} \cdot \begin{bmatrix} X_1 \\ X_2 \\ X_3 \end{bmatrix} + \begin{bmatrix} t_1 \\ t_2 \end{bmatrix} \right) = 0$$

Radial distortion

- Projections $\mathbf{p}$ by the pinhole camera and $\mathbf{p}_d$ by the radially distorted camera lie on the same radial line $\mathbf{l}$.
- The constraint can be written as $\mathbf{l}^T(\mathrm{R}\mathbf{X}+\mathrm{t})=0$

$$\begin{bmatrix} l_1 & l_2 \end{bmatrix} \cdot \left(\begin{bmatrix} R_{11} & R_{12} & R_{13} \\ R_{21} & R_{22} & R_{23} \end{bmatrix} \cdot \begin{bmatrix} X_1 \\ X_2 \\ X_3 \end{bmatrix} + \begin{bmatrix} t_1 \\ t_2 \end{bmatrix} \right) = 0$$

- This is written in matrix form as $\mathbf{l}'^T(\mathrm{R}'\mathbf{X}+\mathrm{t}')=0$

Constraint from radial distortion

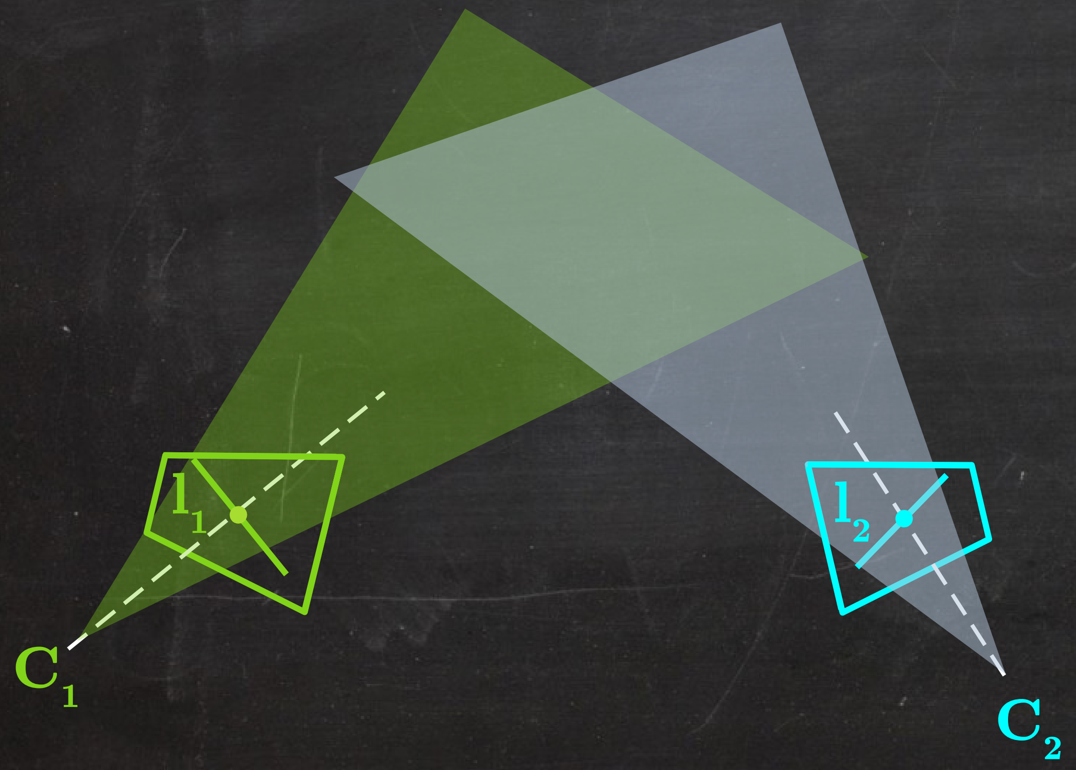

- 2 cameras → $\mathbf{R_i}$, $\mathbf{t_i}$

[1] SriRam Thirthala and Marc Pollefeys: Radial Multi-focal Tensors

Constraint from radial distortion

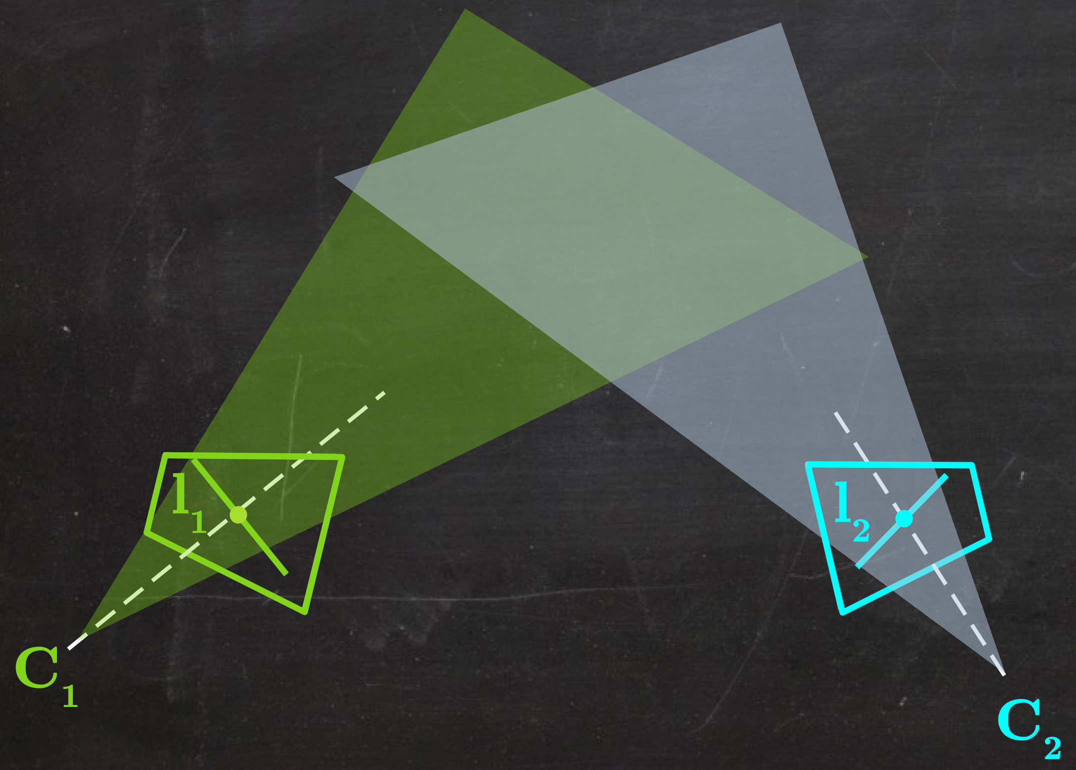

- 2 cameras → $\mathbf{R}_i$, $\mathbf{t}_i$
- Constraint:

$$\exists \mathbf{X}: \mathbf{l'}_1{}^T(R'_1\mathbf{X}+t'_1) = \mathbf{l'}_2{}^T(R'_2\mathbf{X}+t'_2) = 0$$

[1] SriRam Thirthala and Marc Pollefeys: Radial Multi-focal Tensors

Constraint from radial distortion

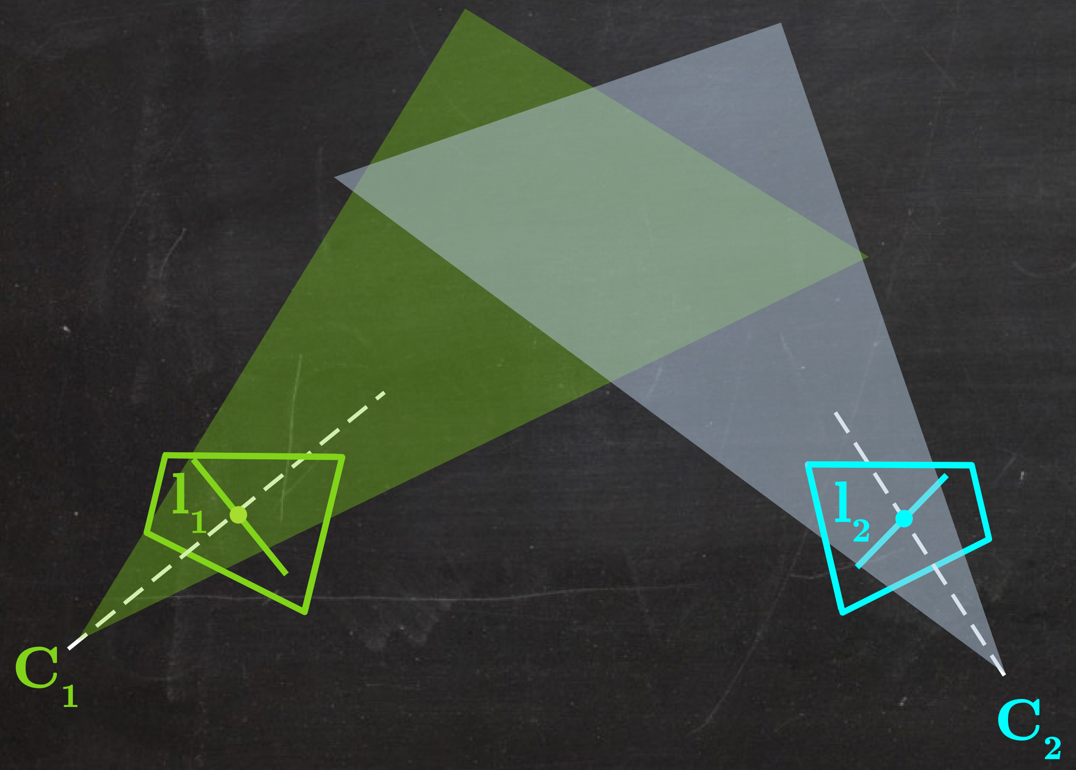

- 2 cameras → $\mathbf{R}_i, \mathbf{t}_i$
- Constraint:

$$\exists \mathbf{X}: \mathbf{l'}_1^T(R'_1\mathbf{X}+t'_1)=\mathbf{l'}_2^T(R'_2\mathbf{X}+t'_2)=0$$

- **2 planes always intersect!**
  - **NO CONSTRAINT!**

[1] SriRam Thirthala and Marc Pollefeys: Radial Multi-focal Tensors

Constraint from radial distortion

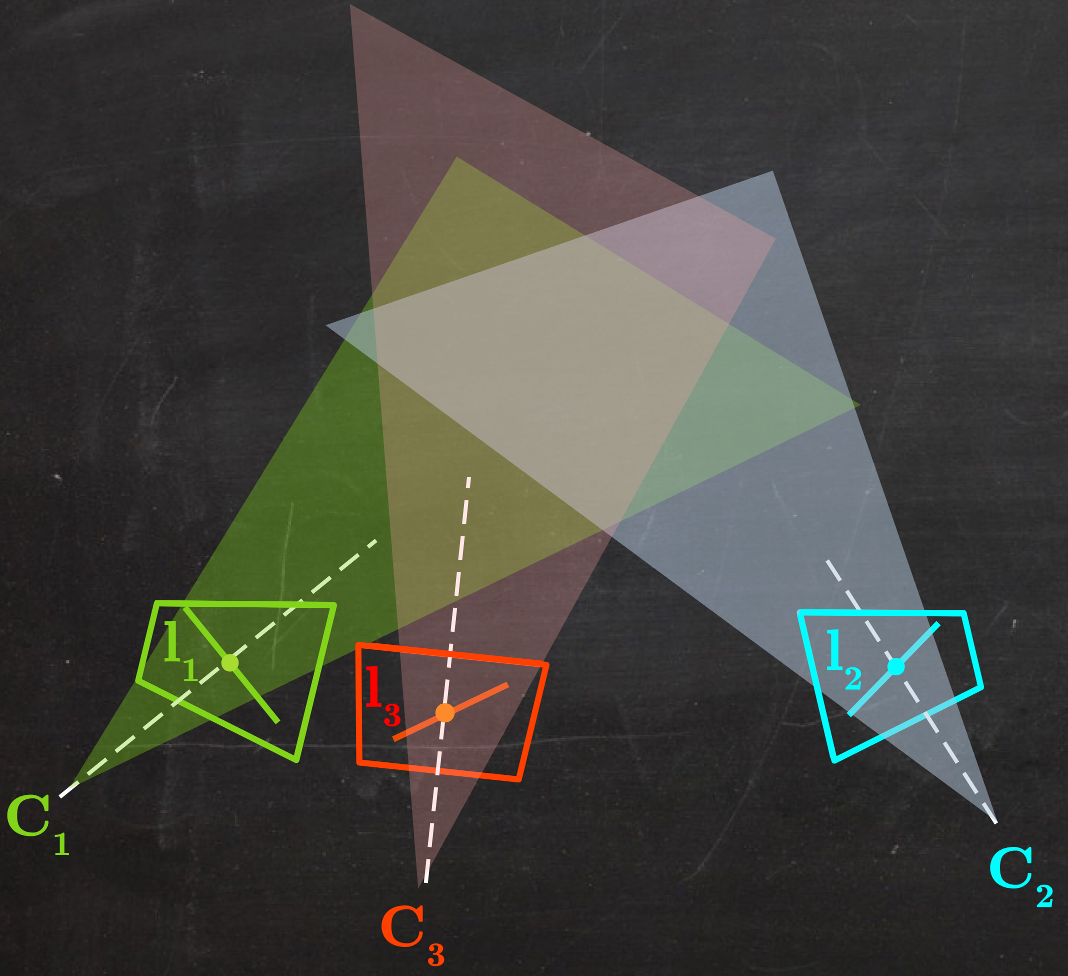

- 3 cameras → $\mathbf{R}_i$, $\mathbf{t}_i$
- Constraint:

$$\exists \mathbf{X}: \mathbf{l'}_1{}^T(R'_1\mathbf{X}+t'_1)=\mathbf{l'}_2{}^T(R'_2\mathbf{X}+t'_2)= \mathbf{l'}_3{}^T(R'_3\mathbf{X}+t'_3)=0$$

[1] SriRam Thirthala and Marc Pollefeys: Radial Multi-focal Tensors

Constraint from radial distortion

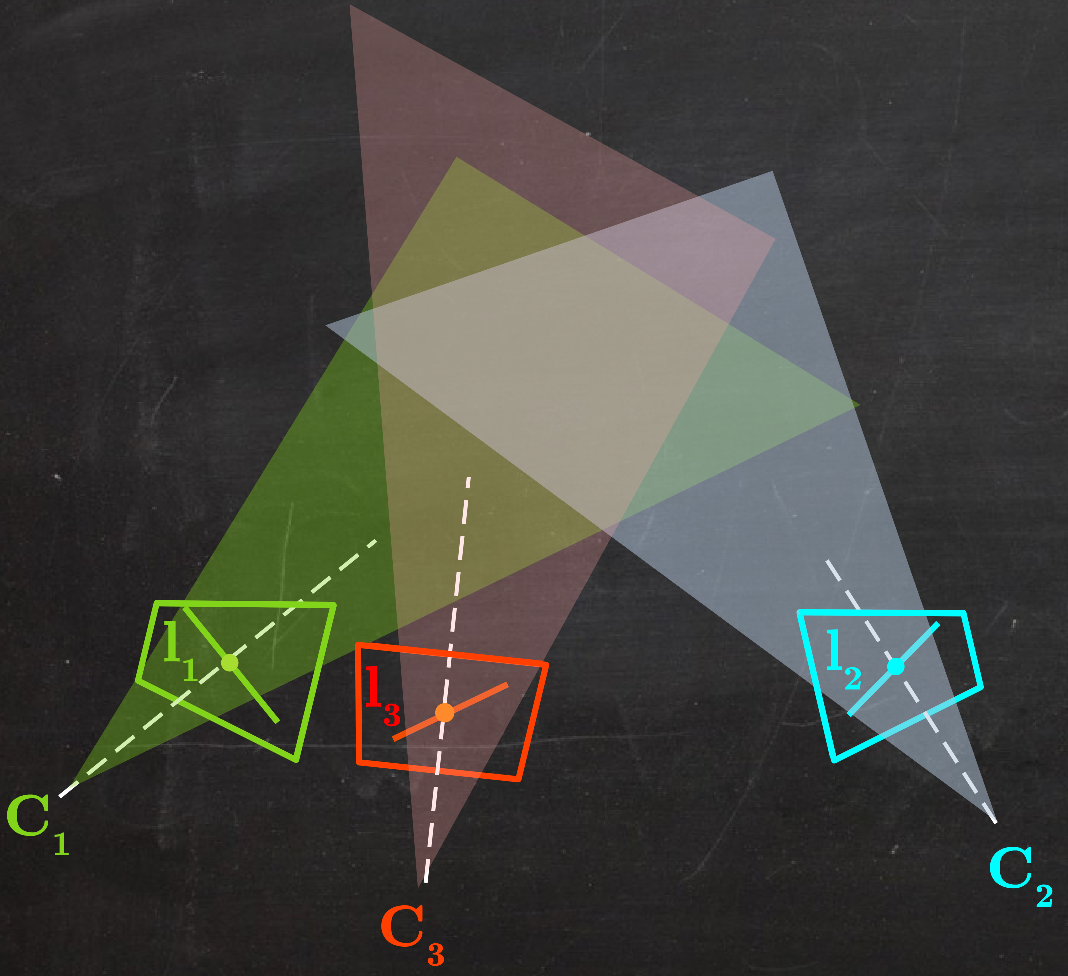

- 3 cameras → $\mathbf{R}_i$, $\mathbf{t}_i$
- Constraint:

$$\exists \mathbf{X}: \mathbf{l'}_1^T(R'_1\mathbf{X}+t'_1)=\mathbf{l'}_2^T(R'_2\mathbf{X}+t'_2)=\mathbf{l'}_3^T(R'_3\mathbf{X}+t'_3)=0$$

- **3 planes always intersect!**
  - **NO CONSTRAINT!**

[1] SriRam Thirthala and Marc Pollefeys: Radial Multi-focal Tensors

Constraint from radial distortion

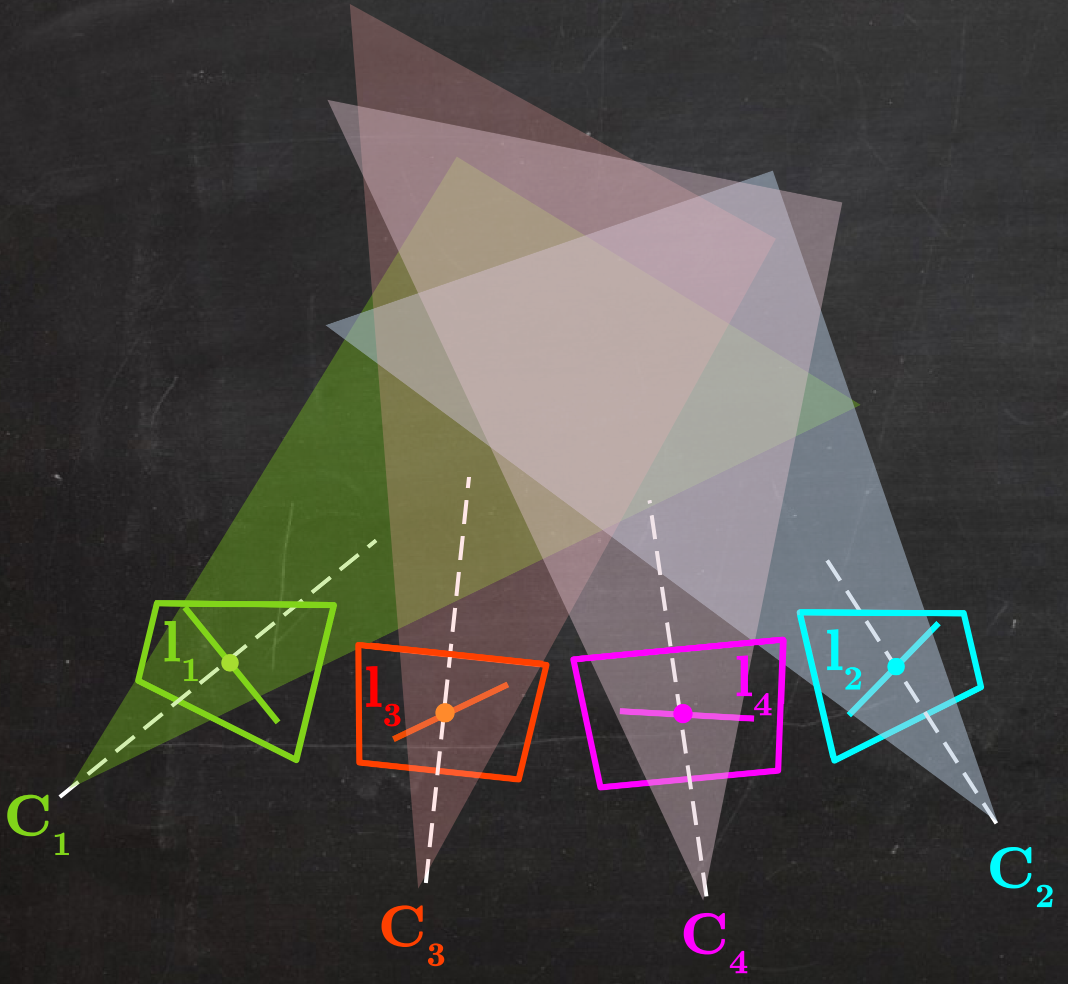

- 4 cameras → $\mathbf{R}_i, \mathbf{t}_i$
- Constraint:

$$\exists \mathbf{X}: \mathbf{l'}_1{}^T(R'_1\mathbf{X}+t'_1)=\mathbf{l'}_2{}^T(R'_2\mathbf{X}+t'_2)=\mathbf{l'}_3{}^T(R'_3\mathbf{X}+t'_3)=\mathbf{l'}_4{}^T(R'_4\mathbf{X}+t'_4)=0$$

[1] SriRam Thirthala and Marc Pollefeys: Radial Multi-focal Tensors

Constraint from radial distortion

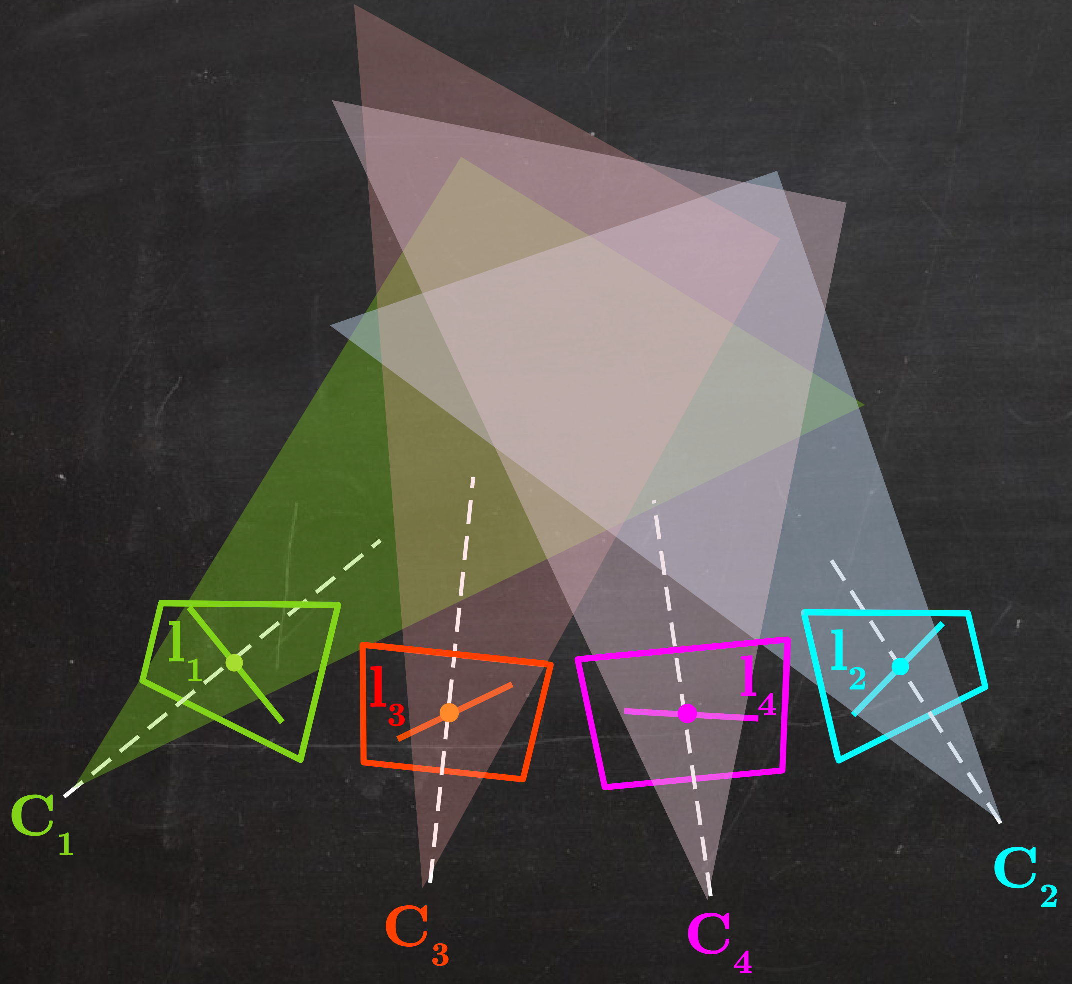

- 4 cameras → $\mathbf{R}_i$, $\mathbf{t}_i$
- Constraint:

$$\exists \mathbf{X}: \mathbf{l'}_1^T(R'_1\mathbf{X}+t'_1)=\mathbf{l'}_2^T(R'_2\mathbf{X}+t'_2)=\mathbf{l'}_3^T(R'_3\mathbf{X}+t'_3)=\mathbf{l'}_4^T(R'_4\mathbf{X}+t'_4)=0$$

- **4 planes generically don't intersect.**

[1] SriRam Thirthala and Marc Pollefeys: Radial Multi-focal Tensors

Constraint from radial distortion

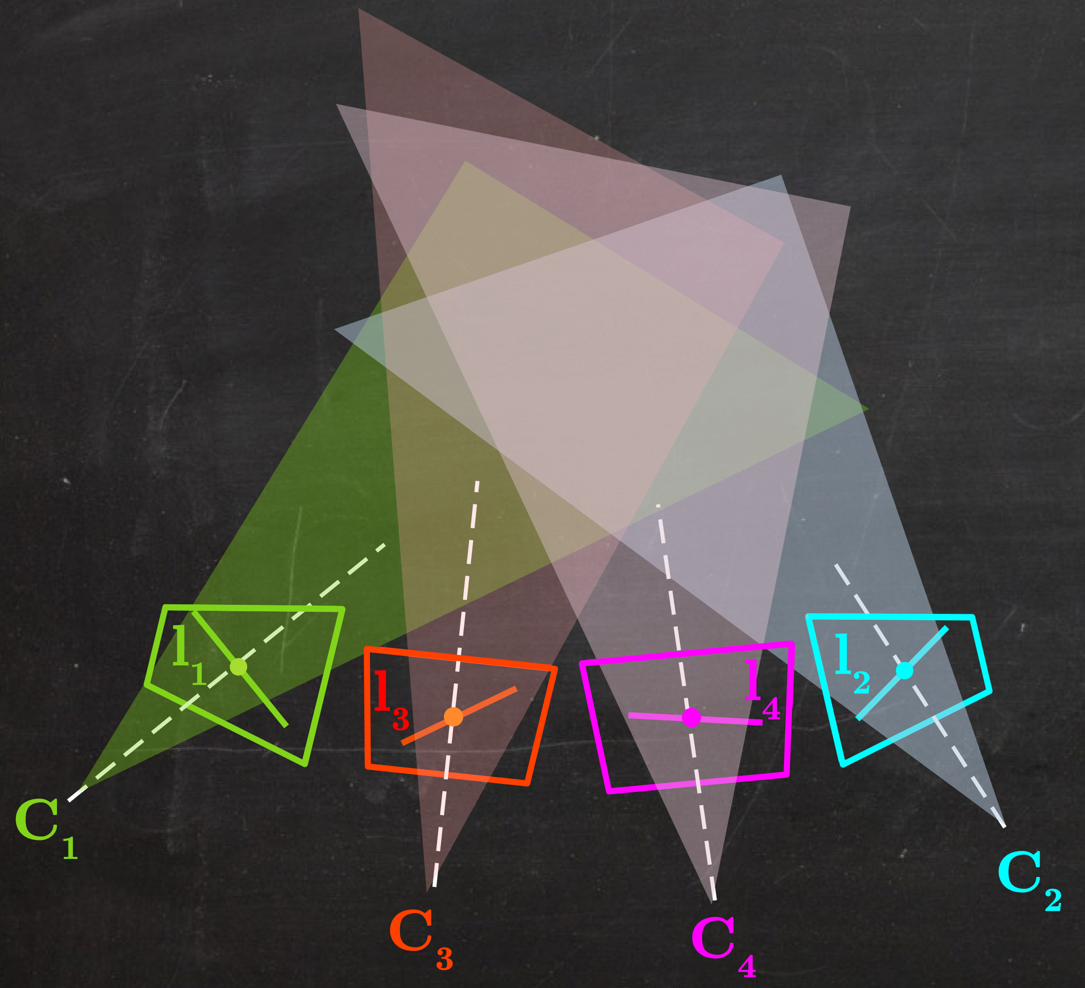

- 4 cameras → $\mathbf{R}_i$, $\mathbf{t}_i$
- Constraint:

$$\exists \mathbf{X}:\ \mathbf{l'}_1^{\,T}(R'_1\mathbf{X}+t'_1)=\mathbf{l'}_2^{\,T}(R'_2\mathbf{X}+t'_2)= \mathbf{l'}_3^{\,T}(R'_3\mathbf{X}+t'_3)=\mathbf{l'}_4^{\,T}(R'_4\mathbf{X}+t'_4)=0$$

- After eliminating $\mathbf{X}$, we get [1]:

$$\Sigma_{i.j.k.l\in\{1,2\}}\mathbf{l'}_{1,i}\mathbf{l'}_{2,j}\mathbf{l'}_{3,k}\mathbf{l'}_{4,l}\mathbf{T}_{i,j,k,l}=0$$

[1] SriRam Thirthala and Marc Pollefeys: Radial Multi-focal Tensors

Constraint from radial distortion

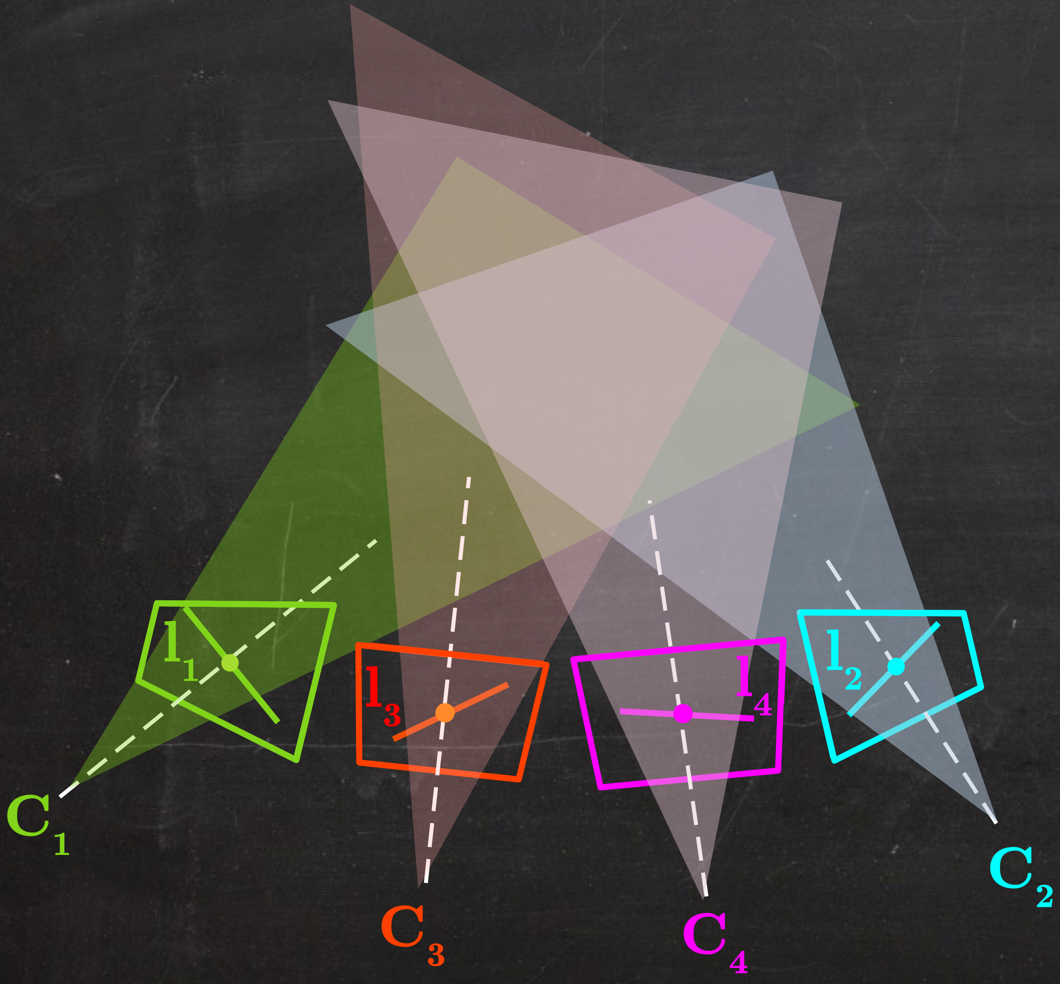

- 4 cameras → $\mathbf{R_i}, \mathbf{t_i}$
- Constraint:

$$\exists \mathbf{X}: \mathbf{l'}_1^T(R'_1\mathbf{X}+t'_1)=\mathbf{l'}_2^T(R'_2\mathbf{X}+t'_2)=$$
$$\mathbf{l'}_3^T(R'_3\mathbf{X}+t'_3)=\mathbf{l'}_4^T(R'_4\mathbf{X}+t'_4)=0$$

- After eliminating $\mathbf{X}$, we get [1]:

$$\mathbf{\Sigma}_{\mathbf{i.j.k.l}\in\{1,2\}}\mathbf{l'}_{1,i}\mathbf{l'}_{2,j}\mathbf{l'}_{3,k}\mathbf{l'}_{4,l}\mathbf{T}_{\mathbf{i,j,k,l}}=\mathbf{0}$$

- Radial quadrifocal tensor [1]:

$$\mathbf{T} \in \mathbb{R}^{2\times2\times2\times2}$$

[1] SriRam Thirthala and Marc Pollefeys: Radial Multi-focal Tensors

General Minimal Problem

- Constraint in form $\Sigma_{i.j.k.l \in \{1,2\}} \mathbf{l'}_{1,i} \mathbf{l'}_{2,j} \mathbf{l'}_{3,k} \mathbf{l'}_{4,l} \mathbf{T}_{i,j,k,l} = \mathbf{0}$
- 4 cameras needed to get one constraint.

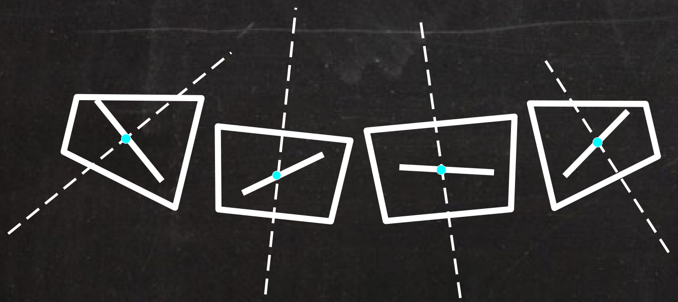

General Minimal Problem

- Constraint in form $\Sigma_{i.j.k.l \in \{1,2\}} \mathbf{l'}_{1,i} \mathbf{l'}_{2,j} \mathbf{l'}_{3,k} \mathbf{l'}_{4,l} \mathbf{T}_{i,j,k,l} = 0$
- 4 cameras needed to get one constraint.
- 4 **uncalibrated cameras** have 13 DoF.

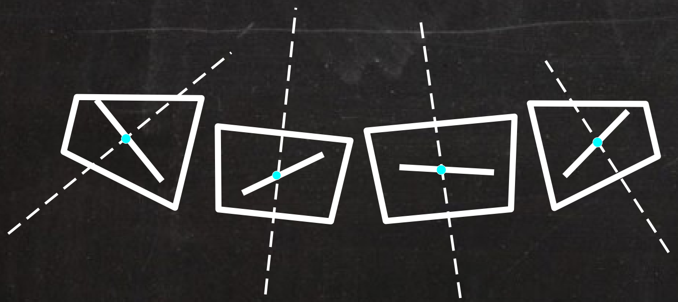

General Minimal Problem

- Constraint in form $\boldsymbol{\Sigma}_{i.j.k.l \in \{1,2\}} \mathbf{l'}_{1,i} \mathbf{l'}_{2,j} \mathbf{l'}_{3,k} \mathbf{l'}_{4,l} \mathbf{T}_{i,j,k,l} = \mathbf{0}$
- 4 cameras needed to get one constraint.
- 4 **uncalibrated cameras** have 13 DoF.
- 4 **calibrated cameras** also have 13 DoF.

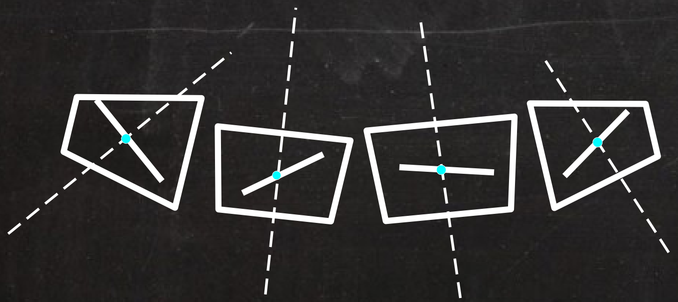

General Minimal Problem

- Constraint in form $\mathbf{\Sigma}_{i.j.k.l\in\{1,2\}}\mathbf{l'}_{1,i}\mathbf{l'}_{2,j}\mathbf{l'}_{3,k}\mathbf{l'}_{4,l}\mathbf{T}_{i,j,k,l}=\mathbf{0}$
- 4 cameras needed to get one constraint.
- 4 **uncalibrated cameras** have 13 DoF.
- 4 **calibrated cameras** also have 13 DoF.
  - 13 correspondences needed to estimate the pose.

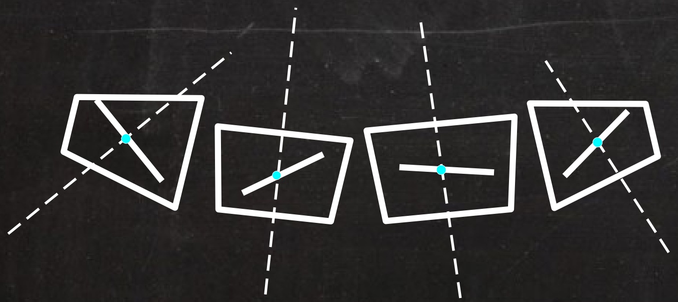

General Minimal Problem

- Constraint in form $\boldsymbol{\Sigma}_{\mathbf{i.j.k.l \in \{1,2\}}} \mathbf{l'}_{1,i} \mathbf{l'}_{2,j} \mathbf{l'}_{3,k} \mathbf{l'}_{4,l} \mathbf{T}_{\mathbf{i,j,k,l}} = \mathbf{0}$
- 4 cameras needed to get one constraint.
- 4 **uncalibrated cameras** have 13 DoF.
- 4 **calibrated cameras** also have 13 DoF.
  - 13 correspondences needed to estimate the pose.
- The minimal problem has 3584 complex solutions.

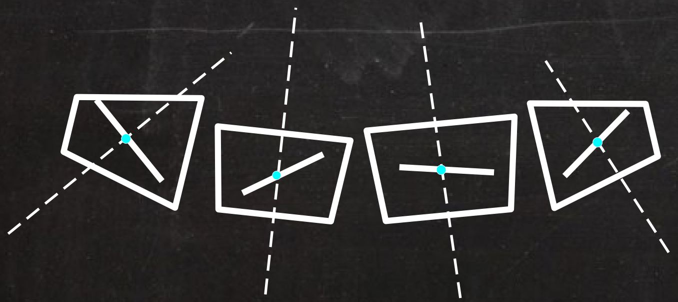

Internal Constraints

- Radial Quadrifocal tensor (RQT) $\mathbf{T}$ with shape $2 \times 2 \times 2 \times 2$

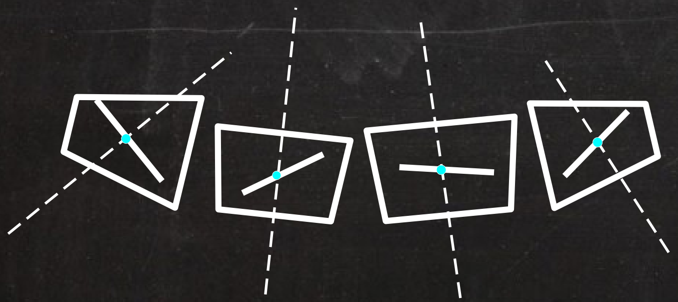

Internal Constraints

- Radial Quadrifocal tensor (RQT) $\mathbf{T}$ with shape $2\times2\times2\times2$
  - Elements of $\mathbf{T}$ are functions of $\mathbf{R_i}$, $\mathbf{t_i}$: it has **13 DoF**

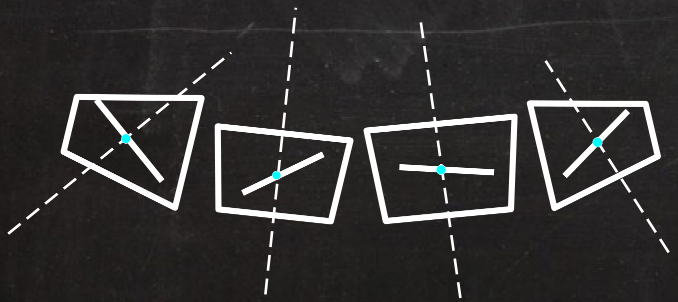

Internal Constraints

- Radial Quadrifocal tensor (RQT) $\mathbf{T}$ with shape $2\times2\times2\times2$
  - Elements of $\mathbf{T}$ are functions of $\mathbf{R_i}$, $\mathbf{t_i}$: it has **13 DoF**
  - space of all $2\times2\times2\times2$ tensors has **15 DoF** up to scale

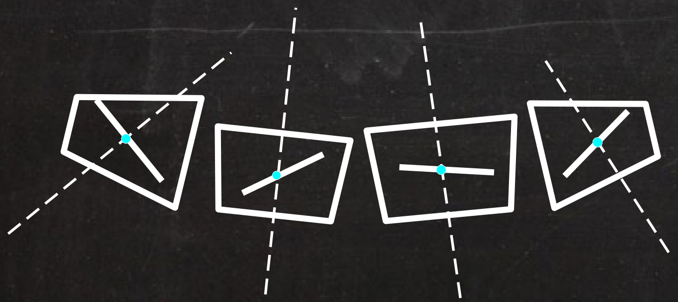

Internal Constraints

- Radial Quadrifocal tensor (RQT) $\mathbf{T}$ with shape $2\times2\times2\times2$
  - Elements of $\mathbf{T}$ are functions of $\mathbf{R_i}$, $\mathbf{t_i}$: it has **13 DoF**
  - space of all $2\times2\times2\times2$ tensors has **15 DoF** up to scale
- Set of all RQTs: 13 dimensional variety 15D space

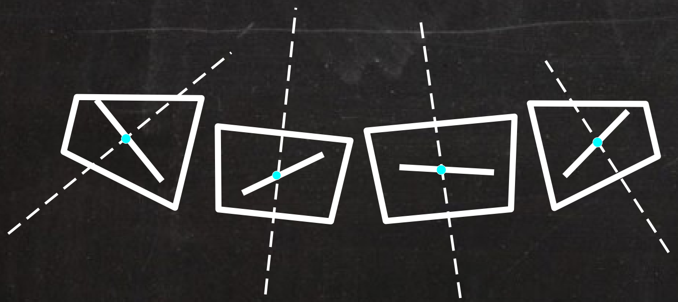

Internal Constraints

- Radial Quadrifocal tensor (RQT) $\mathbf{T}$ with shape $2\times2\times2\times2$
  - Elements of $\mathbf{T}$ are functions of $\mathbf{R_i}$, $\mathbf{t_i}$: it has **13 DoF**
  - space of all $2\times2\times2\times2$ tensors has **15 DoF** up to scale
- Set of all RQTs: 13 dimensional variety 15D space
  - Locally defined by 2 constraints

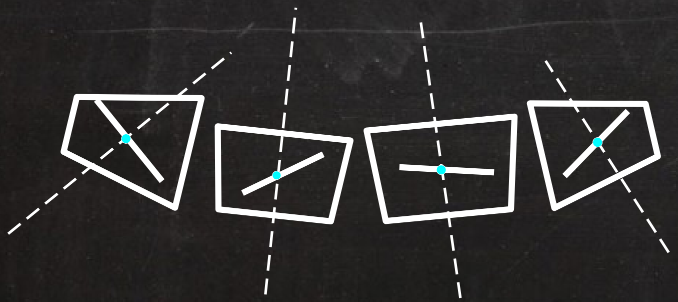

Internal Constraints

- Radial Quadrifocal tensor (RQT) $\mathbf{T}$ with shape $2\times2\times2\times2$
  - Elements of $\mathbf{T}$ are functions of $\mathbf{R_i}$, $\mathbf{t_i}$: it has **13 DoF**
  - space of all $2\times2\times2\times2$ tensors has **15 DoF** up to scale
- Set of all RQTs: 13 dimensional variety 15D space
  - Locally defined by 2 constraints
  - Globally defined by 718 constraints of degree 12

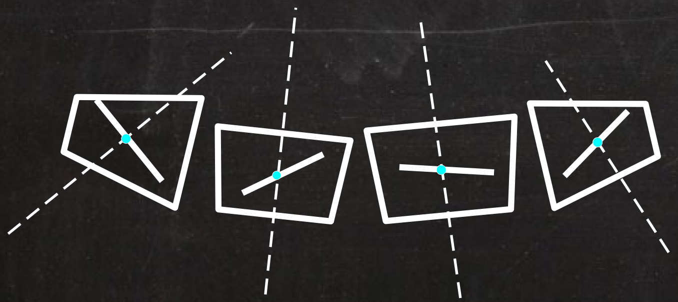

Problem Symmetries

- Problem Symmetries:
  - Revealed by *Galois Group* [1] of the problem.

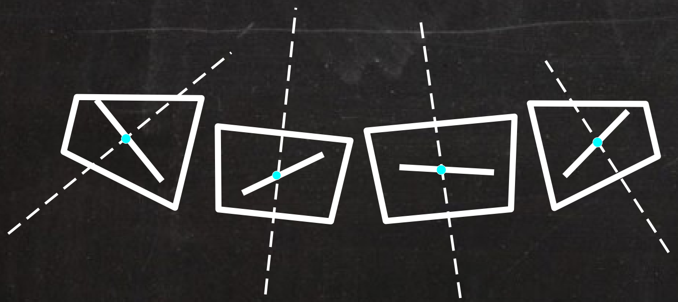

[1] T. Duff, V. Korotynskiy, T. Pajdla, and M. H. Regan, Galois/monodromy groups for decomposing minimal problems in 3D reconstruction, SIAM Journal on Applied Algebra and Geometry, 2022.

Problem Symmetries

- Problem Symmetries:
  - Revealed by *Galois Group* [1] of the problem.
  - The *Galois Group* can be computed using *Monodromy*.

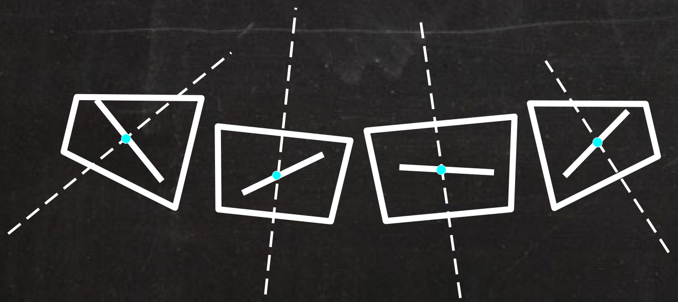

[1] T. Duff, V. Korotynskiy, T. Pajdla, and M. H. Regan, Galois/monodromy groups for decomposing minimal problems in 3D reconstruction, SIAM Journal on Applied Algebra and Geometry, 2022.

Problem Symmetries

- Problem Symmetries:
  - Revealed by *Galois Group* [1] of the problem.
  - The *Galois Group* can be computed using *Monodromy*.
- The problem has 3584 solutions.
- It decomposes into subproblems of 28, 2, 4, and 2^4 solutions.

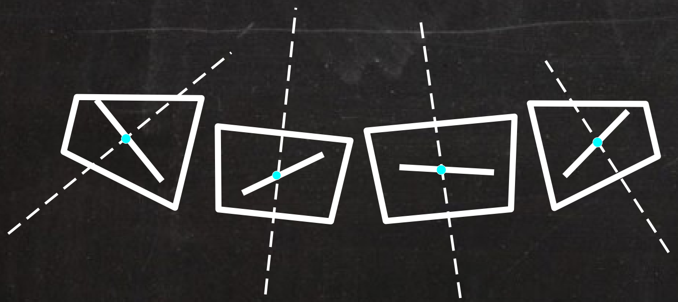

[1] T. Duff, V. Korotynskiy, T. Pajdla, and M. H. Regan, Galois/monodromy groups for decomposing minimal problems in 3D reconstruction, SIAM Journal on Applied Algebra and Geometry, 2022.

Problem Symmetries

- Problem Symmetries:
  - Revealed by *Galois Group* [1] of the problem.
  - The *Galois Group* can be computed using *Monodromy*.
- The problem has 3584 solutions.
- It decomposes into subproblems of 28, 2, 4, and 2^4 solutions.
- Effective reduction of the number of solutions.
  - significant simplification of the problem

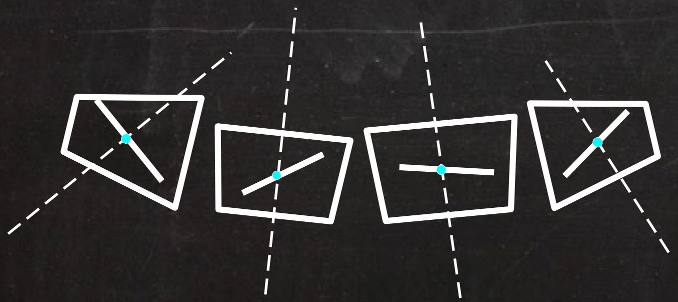

[1] T. Duff, V. Korotynskiy, T. Pajdla, and M. H. Regan, Galois/monodromy groups for decomposing minimal problems in 3D reconstruction, SIAM Journal on Applied Algebra and Geometry, 2022.

Problem Symmetries

2 Pinhole Cameras, 5 Points

4 Radial Cameras, 13 Points

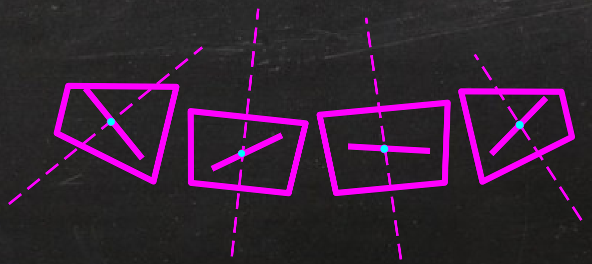

Problem Symmetries

2 Pinhole Cameras, 5 Points

- 40 solutions in terms of $\mathbf{R}, \mathbf{t}$

4 Radial Cameras, 13 Points

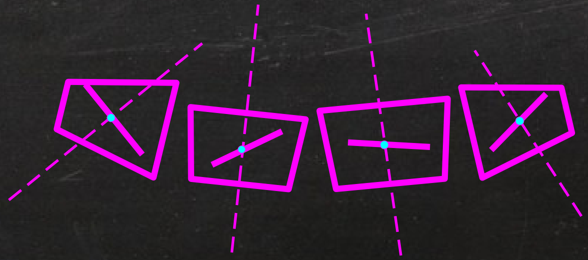

Problem Symmetries

2 Pinhole Cameras, 5 Points

- 40 solutions in terms of $\mathbf{R}, \mathbf{t}$
- Subproblems of 10 and 4 solutions

4 Radial Cameras, 13 Points

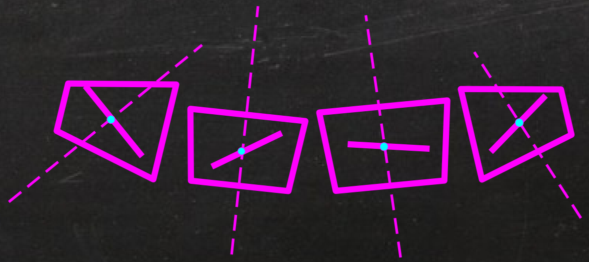

Problem Symmetries

2 Pinhole Cameras, 5 Points

- 40 solutions in terms of $\mathbf{R}, \mathbf{t}$
- Subproblems of 10 and 4 solutions
- Every instance has 10 solutions in terms of essential matrices $\mathbf{E}$

4 Radial Cameras, 13 Points

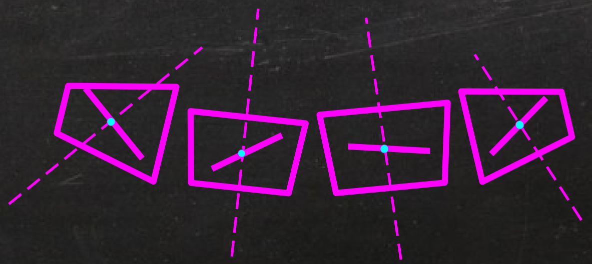

Problem Symmetries

2 Pinhole Cameras, 5 Points

- 40 solutions in terms of $\mathbf{R}, \mathbf{t}$
- Subproblems of 10 and 4 solutions
- Every instance has 10 solutions in terms of essential matrices $\mathbf{E}$
- Every $\mathbf{E}$ has 4 decompositions to $\mathbf{R}, \mathbf{t}$

4 Radial Cameras, 13 Points

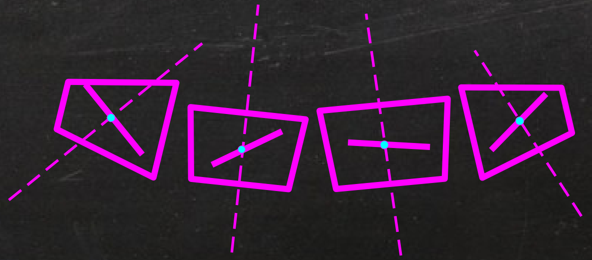

Problem Symmetries

2 Pinhole Cameras, 5 Points

- 40 solutions in terms of $\mathbf{R}, \mathbf{t}$
- Subproblems of 10 and 4 solutions
- Every instance has 10 solutions in terms of essential matrices $\mathbf{E}$
- Every $\mathbf{E}$ has 4 decompositions to $\mathbf{R}, \mathbf{t}$

4 Radial Cameras, 13 Points

- 3584 solutions in terms of $\mathbf{R_i}, \mathbf{t_i}$

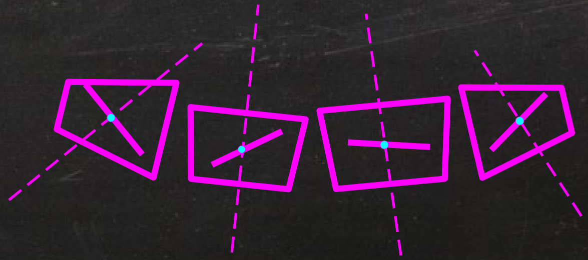

Problem Symmetries

2 Pinhole Cameras, 5 Points

- 40 solutions in terms of $\mathbf{R}, \mathbf{t}$
- Subproblems of 10 and 4 solutions
- Every instance has 10 solutions in terms of essential matrices $\mathbf{E}$
- Every $\mathbf{E}$ has 4 decompositions to $\mathbf{R}, \mathbf{t}$

4 Radial Cameras, 13 Points

- 3584 solutions in terms of $\mathbf{R_i}, \mathbf{t_i}$
- Subproblems of 28, 2, 4, 2^4 solutions

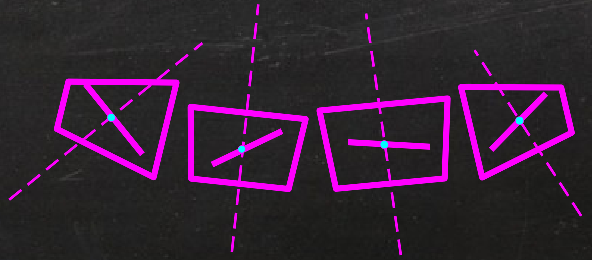

Problem Symmetries

2 Pinhole Cameras, 5 Points

- 40 solutions in terms of $\mathbf{R}, \mathbf{t}$
- Subproblems of 10 and 4 solutions
- Every instance has 10 solutions in terms of essential matrices $\mathbf{E}$
- Every $\mathbf{E}$ has 4 decompositions to $\mathbf{R}, \mathbf{t}$

4 Radial Cameras, 13 Points

- 3584 solutions in terms of $\mathbf{R}_\mathrm{i}, \mathbf{t}_\mathrm{i}$
- Subproblems of 28, 2, 4, 2^4 solutions
- Every instance has 28 solutions in terms of $\mathbf{T}$

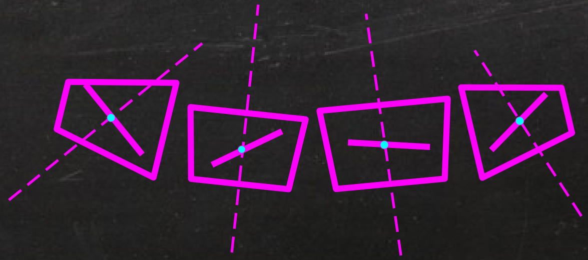

Problem Symmetries

2 Pinhole Cameras, 5 Points

- 40 solutions in terms of $\mathbf{R}, \mathbf{t}$
- Subproblems of 10 and 4 solutions
- Every instance has 10 solutions in terms of essential matrices $\mathbf{E}$
- Every $\mathbf{E}$ has 4 decompositions to $\mathbf{R}, \mathbf{t}$

4 Radial Cameras, 13 Points

- 3584 solutions in terms of $\mathbf{R}_\mathrm{i}, \mathbf{t}_\mathrm{i}$
- Subproblems of 28, 2, 4, 2^4 solutions
- Every instance has 28 solutions in terms of $\mathbf{T}$
- Every $\mathbf{T}$ has 128 decompositions to $\mathbf{R}_\mathrm{i}, \mathbf{t}_\mathrm{i}$

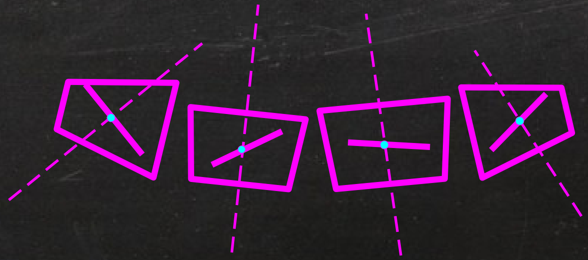

Upright minimal problem

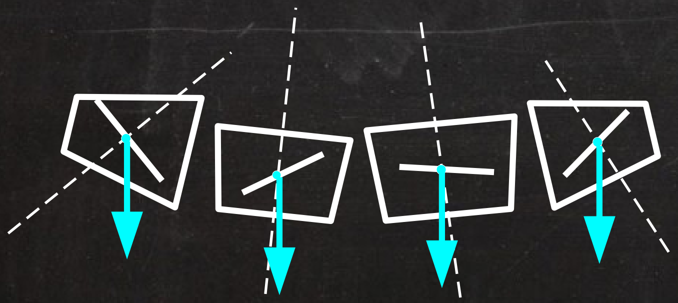

Upright minimal problem

- 4 cameras needed to get one constraint.

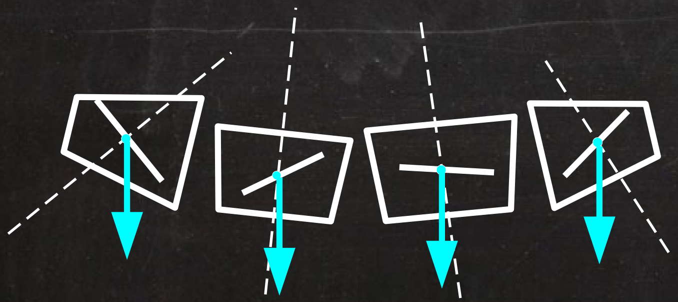

Upright minimal problem

- 4 cameras needed to get one constraint.
- 4 **upright cameras** have 7 DoF.

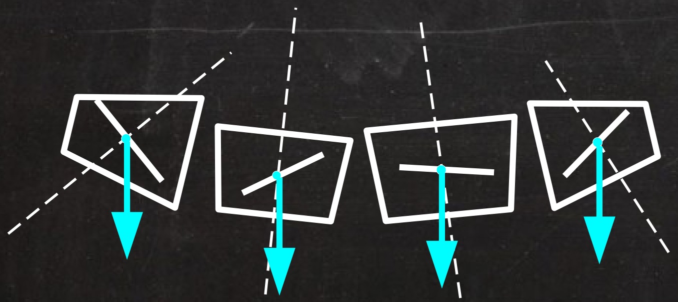

Upright minimal problem

- 4 cameras needed to get one constraint.
- 4 **upright cameras** have 7 DoF.
  - 7 correspondences needed to estimate the RQT.

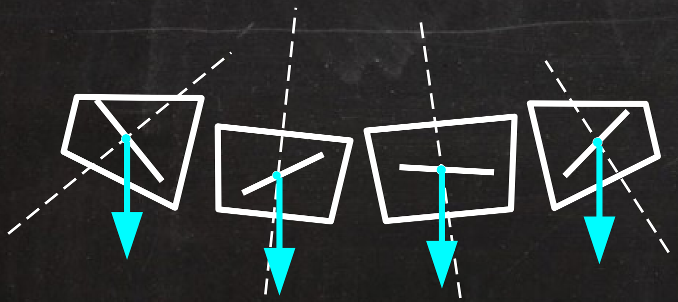

Upright minimal problem

- 4 cameras needed to get one constraint.
- 4 **upright cameras** have 7 DoF.
  - 7 correspondences needed to estimate the RQT.
- The minimal problem has 50 complex solutions.
  - It has subproblems with 25 and 2 solutions.

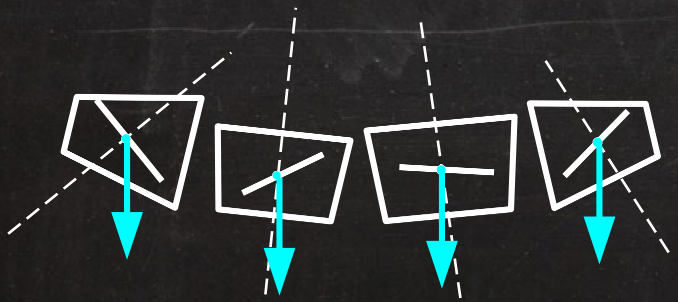

Minimal Solvers

- Solved by **Homotopy Continuation**

Minimal Solvers

- Solved by **Homotopy Continuation**
- **General case**

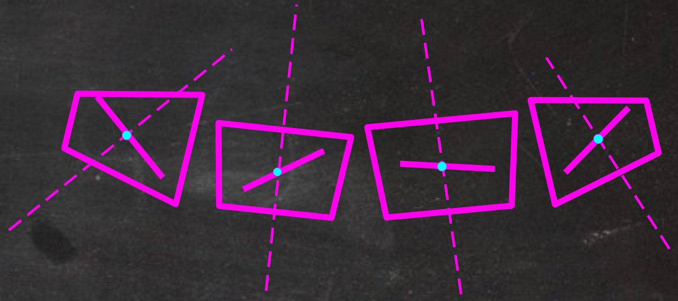

- **Upright case**

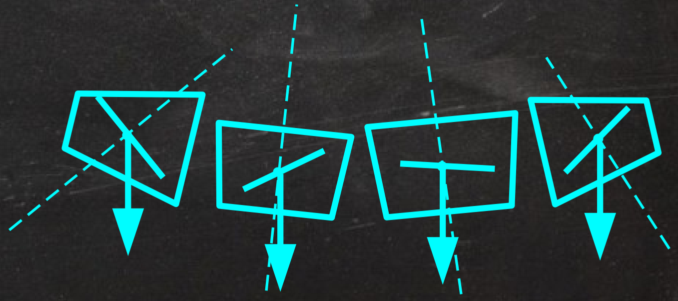

Minimal Solvers

- Solved by **Homotopy Continuation**
- **General case**
  - 28 homotopy paths
  - Metric upgrade to get all solutions
  - Runtime: 78 ms

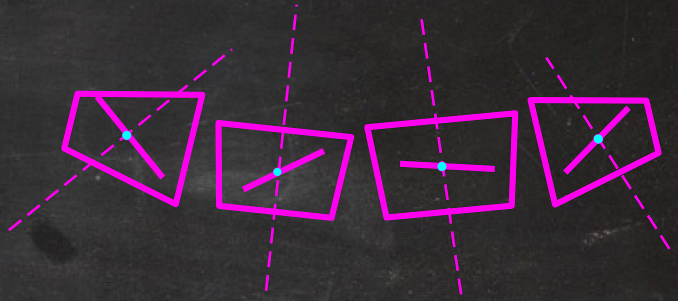

- **Upright case**

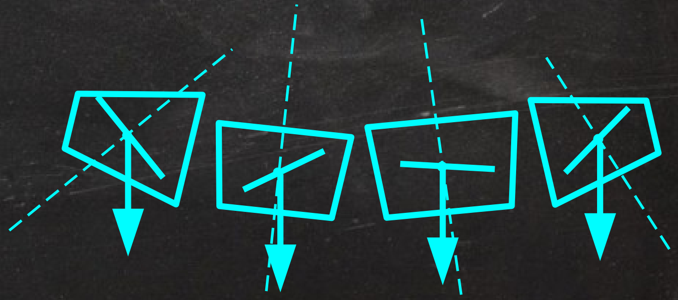

Minimal Solvers

- Solved by **Homotopy Continuation**
- **General case**
  - 28 homotopy paths
  - Metric upgrade to get all solutions
  - Runtime: 78 ms

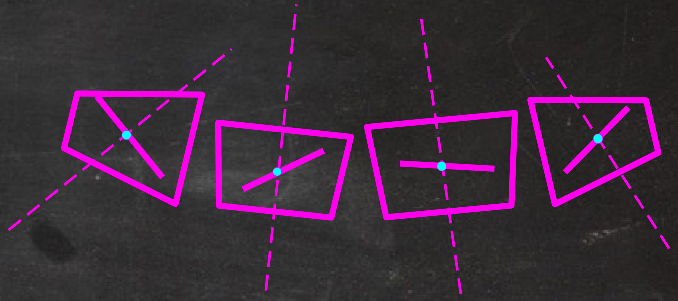

- **Upright case**
  - 25 homotopy paths
  - Runtime: 18 ms

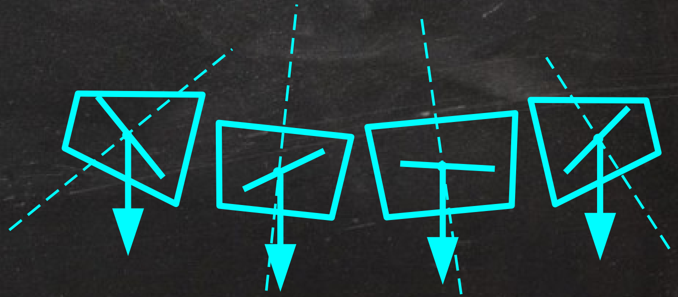

Results

- Comparison with Larsson et al. [1]
- *Left:* general quadruplets

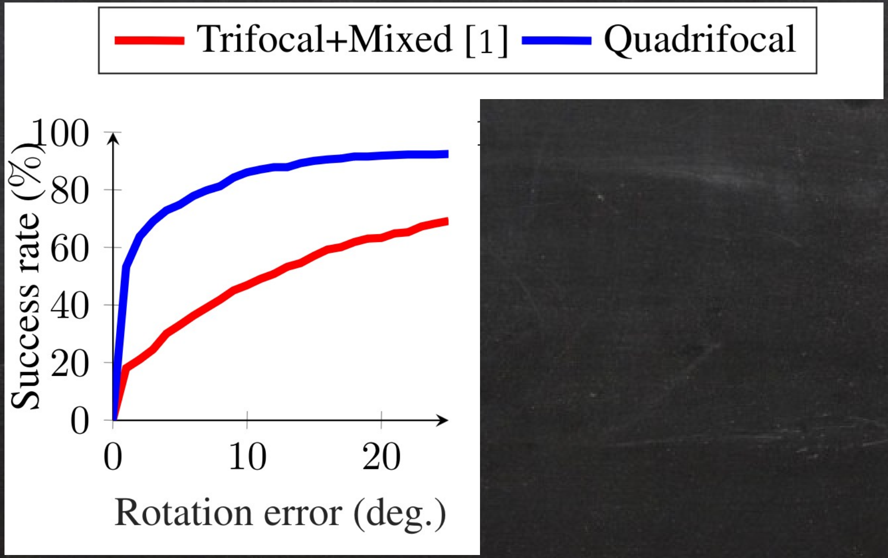

[1] Calibration-free Structure-from-Motion with Calibrated Radial Trifocal Tensors, V. Larsson, N. Zobernig, K. Taskin, M. Pollefeys

Results

- Comparison with Larsson et al. [1]
- *Left:* general quadruplets
- *Right:* quadruplets selected by an expensive heuristic [1]

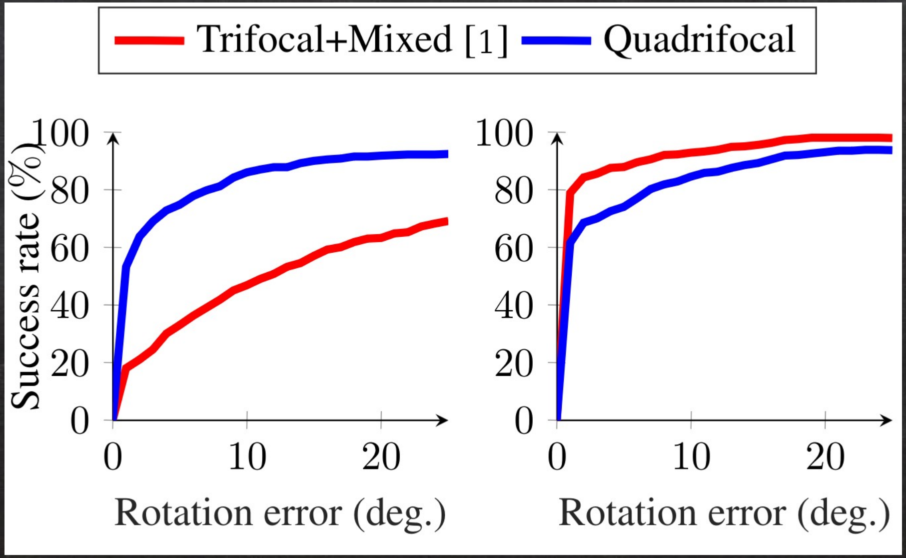

[1] Calibration-free Structure-from-Motion with Calibrated Radial Trifocal Tensors, V. Larsson, N. Zobernig, K. Taskin, M. Pollefeys

Result Kirchenge

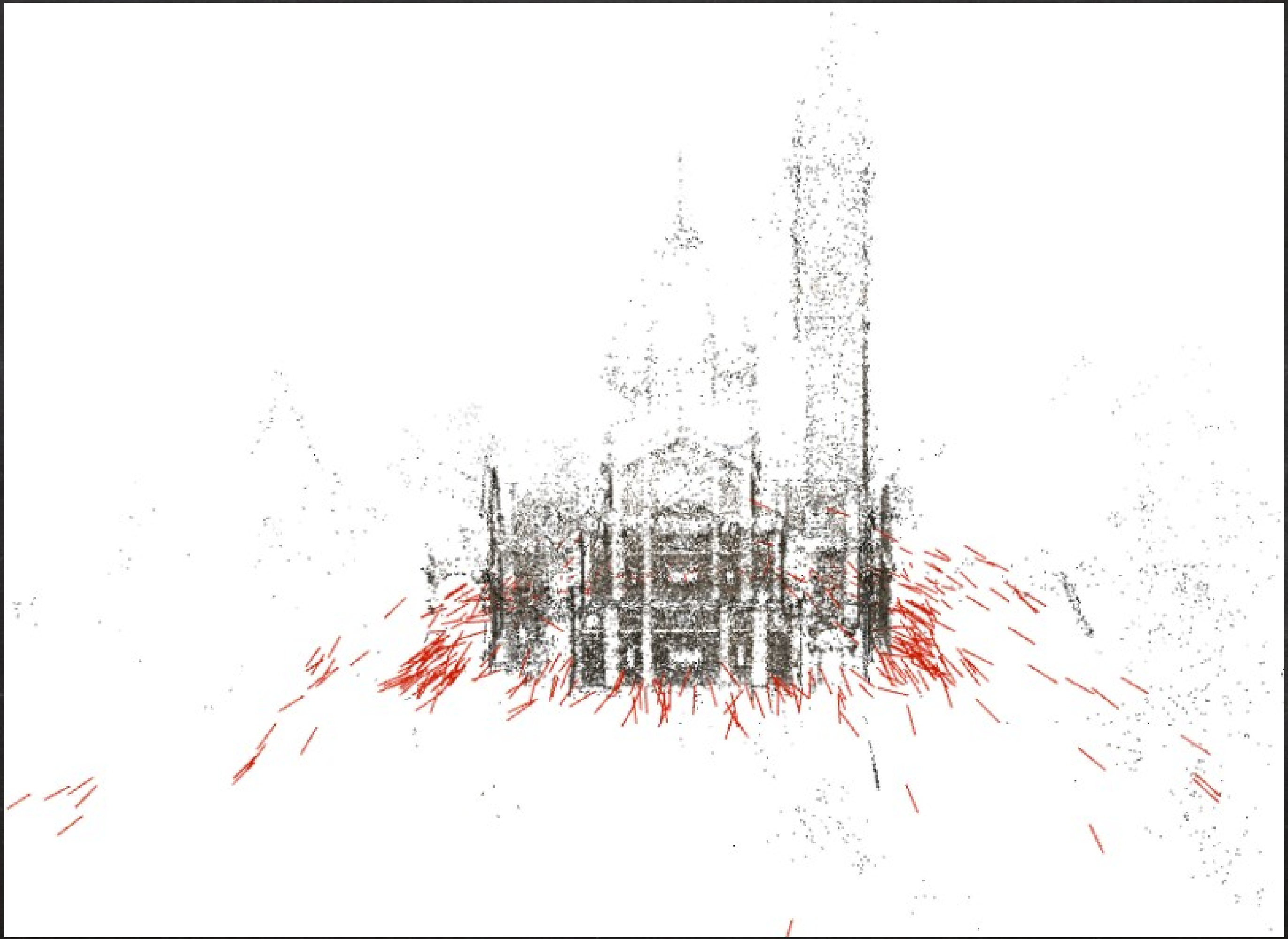

Results (Eglise)

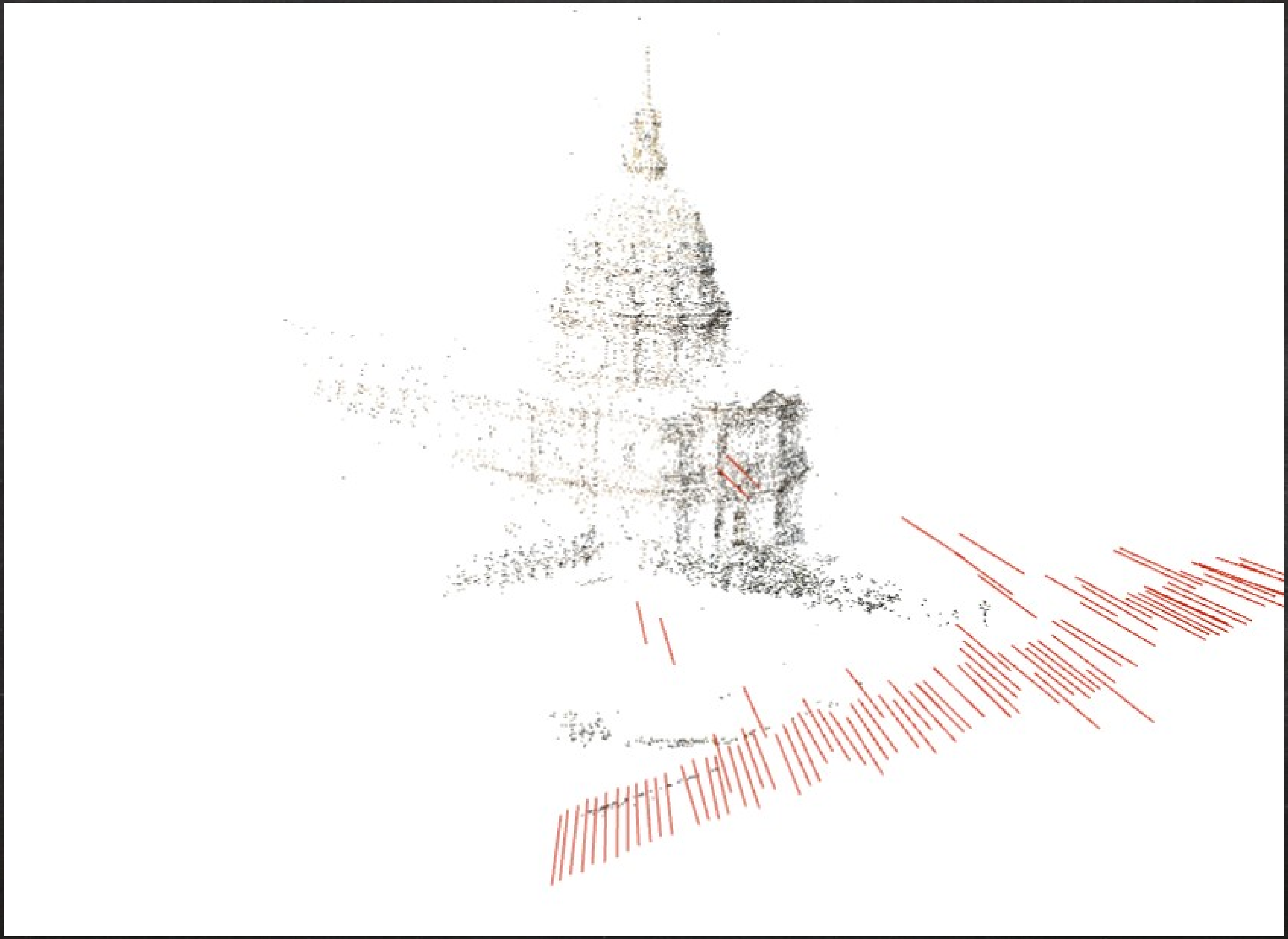

Results (Door)

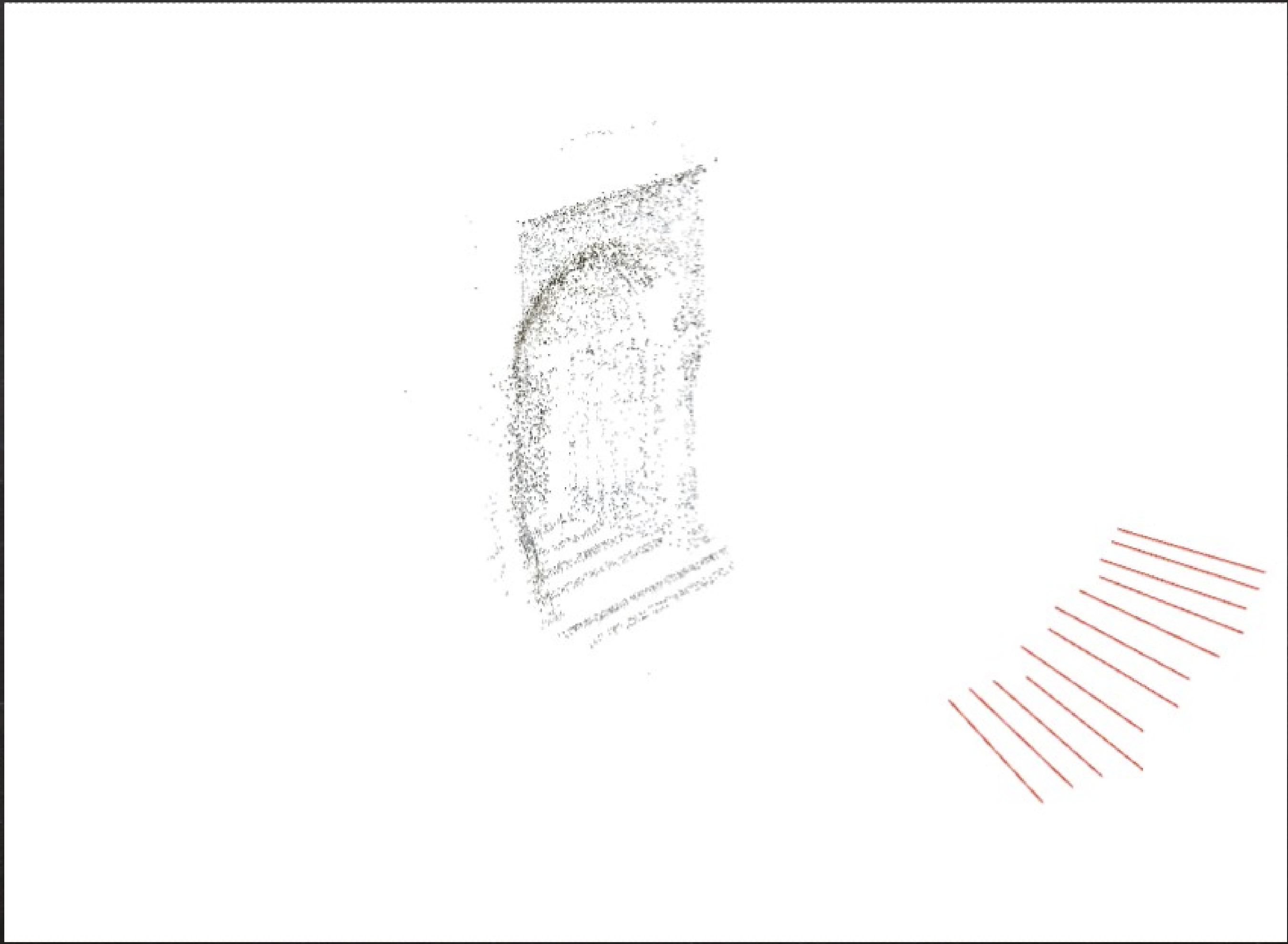

THE END

Visit us at **WED-AM-073**